Journal of Medicinal Chemistry

Article

Novel C-4 Heteroaryl 13-Cis Retinamide Mnk/AR Degrading Agents Inhibit Cell Proliferation and Migration and Induce Apoptosis in Human Breast and Prostate Cancer Cells and Suppress Growth of MDA-MB-231 Human Breast and CWR22Rv1 Human Prostate Tumor Xenografts in Mice

Hannah W. Mbatia, Senthilmurugan Ramalingam, Vidya P Ramamurthy, Marlena S Martin, Andrew K. Kwegyir-Afful, and Vincent C. O. Njar

J. Med. Chem., **Just Accepted Manuscript** • DOI: 10.1021/jm501792c • Publication Date (Web): 29 Jan 2015

Just Accepted

Journal of Medicinal Chemistry is published by the American Chemical Society. 1155 Sixteenth Street N.W., Washington, DC 20036

Novel C-4 Heteroaryl 13-Cis Retinamide Mnk/AR Degrading Agents Inhibit Cell Proliferation and Migration and Induce Apoptosis in Human Breast and Prostate Cancer Cells and Suppress Growth of MDA-MB-231 Human Breast and CWR22Rv1 Human Prostate Tumor Xenografts in Mice

Hannah W. Mbatia[1,2,#], Senthilmurugan Ramalingam[1,2,#], Vidya P. Ramamurthy[1,2,#], Marlena S. Martin[1,2,¥], Andrew K. Kwegyir-Afful[1,2] and Vincent C. O. Njar[1,2,3,*]

[1]Department of Pharmacology, [2]Center for Biomolecular Therapeutics, Maryland, [3]Marlene Stewart Greenebaum Cancer Center, University of Maryland School of Medicine, 685 West Baltimore Street, Baltimore, MD 21201-1559, USA.

[¥] Current Address: Bernard J. Dunn School of Pharmacy, Shenandoah University, 45085 University Drive, Suite 202, Ashburn, VA 20147

ABSTRACT

The synthesis and *in vitro* and *in vivo* anti-breast and anti-prostate cancers activities of novel C-4 heteroaryl 13-cis retinamides that modulate Mnk-eIF4E and AR signaling are discussed. Modifications of the C-4 heteroaryl substituents reveal that the 1*H*-imidazole is essential for high anti-cancer activity. The most potent compounds against a variety of human breast and prostate cancer (BC/PC) cell lines were compounds **16** (VNHM-1-66), **20** (VNHM-1-81) and **22** (VNHM-1-73). In these cell lines; the compounds induce Mnk1/2 degradation to substantially suppress eIF4E phosphorylation. In PC cells, the compounds induce degradation of both full-length androgen receptor (fAR) and splice variant AR (AR-V7) to inhibit AR transcriptional activity. More importantly, VNHM-1-81 has strong *in vivo* anti-breast and anti-prostate cancer activities, while VNHM-1-73 exhibited strong *in vivo* anti-breast cancer activity, with no apparent host toxicity. Clearly, these lead compounds are strong candidates for development for the treatments of human breast and prostate cancers.

INTRODUCTION

Disruption and/or perturbation of cap-dependent translation is essential for the development of cancers and many fibrotic diseases, the most notable being Alzheimer's disease.[1] Hyper-activation of eukaryotic translation initiation factor 4E (eIF4E), the mRNA 5' cap-binding protein of cap-dependent translation promotes exquisite transcript-specific translation of key mRNAs that are indispensable in cancer initiation, progression and metastases.[2] The oncogenic potential of eIF4E is dependent on serine 209 phosphorylation by MAPK-interacting kinases 1 and 2 (Mnk1/2). Currently, there are several strategies, directed at disruption of the eukaryotic initiation factor 4F (eIF4F) complex to inhibit hyper-activity of oncogenic protein translation as a means to effectively treat a variety of cancers.[3]

When targeting a critical process such as translation, **a major critical question** is whether the drug will have significant effects on normal cellular processes, leading to limiting toxicities and too narrow a therapeutic window. This question has been addressed by several experimental and a few clinical studies. Recently, Graff and colleagues elegantly demonstrated that down-regulation of eIF4E by antisense oligonucleotide therapy caused reduction of *in vivo* tumor growth in MDA-MB-231 breast and PC-3 prostate cancer models without toxicity despite an ~80% eIF4E knockdown in essential organs.[4] These data provided *in vivo* evidence that cancers may be more susceptible to eIF4E inhibition than normal tissue and provided the basis for advancement of eIF4E-specific antisense molecule LY2275796 into Phase 1 clinical studies.[5] In other more recent studies, cercosporamide, a potent Mnk1/2 kinase inhibitor was reported to exhibit antitumor efficacies against HCT116 colon carcinoma xenograft tumors[6] and MV4-11 acute myeloid leukemia (AML) tumors in animal models,[7] without any toxicity.

We previously reported that our proprietary novel C-4 azolyl retinamides (NRs) based on all-*trans* retinoic acid (ATRA) (**1**) (**Figure 1**) scaffold induced apoptosis, potently inhibited the growth, migration and invasion of a variety of human breast and prostate cancer cell lines.[8] With respect to the breast cancer cell lines, we demonstrated that the anti-breast cancer activity of our NRs was due mainly to degradation of Mnk1/2 with subsequent suppression of phosphorylated eIF4E (peIF4E).[8a] However, in the prostate cancer (PC) cell lines, we demonstrated that the anti-tumor activity of the NRs was due to simultaneous inhibition of the Mnk/eIF4E and androgen receptor (AR) signaling pathways.[8b] It is important to state here that unlike other reported small molecules which inhibit Mnk1/2 kinase activities,[3e, 6, 9] our NRs induced Mnk1/2 degradation via the ubiquitin-proteasome pathway with resultant depletion of peIF4E.[8] The structures of promising Mnk 1 and/or 2 kinase inhibitors, including CGP57380 (**2**),[10] cercosporamide (**3**),[6] MNKI-19 (**4**)[11] and MNKI85 (**5**)[11] are presented in **Figure 1**. In addition, the structures of our lead Mnk degrading agent (MNKDA), **VNLG-152** (**6**)[8a] and related compounds,[12 12] **VN/14-1** (**7**), **VN/66-1** (**8**) and *N*-(4-hydroxyphenyl) retinamide (4-HPR or fenretinide) (**9**) are also depicted in **Figure 1**.

In the present study, we have synthesized novel compounds based on 13-*cis* retinoic acid (13-CRA) (**10**) (**Figure 1)** scaffold, and their anti-cancer activities were evaluated in both *in vitro* and *in vivo* models of human breast and prostate cancers. These novel compounds target Mnk1/2 degradation in both breast cancer and PC cells and also induce AR degradation in PC cells, which in turn led to induction of apoptosis, cell cycle arrest, inhibition of cell growth, colonization, migration, and invasion. Importantly, compounds **20** and **22** significantly inhibited tumor growth of aggressive MDA-MB-213 breast cancer xenografts, while **20** was shown to substantially suppress castration-resistant prostate cancer CWR2Rv1 xenografts *in vivo*.

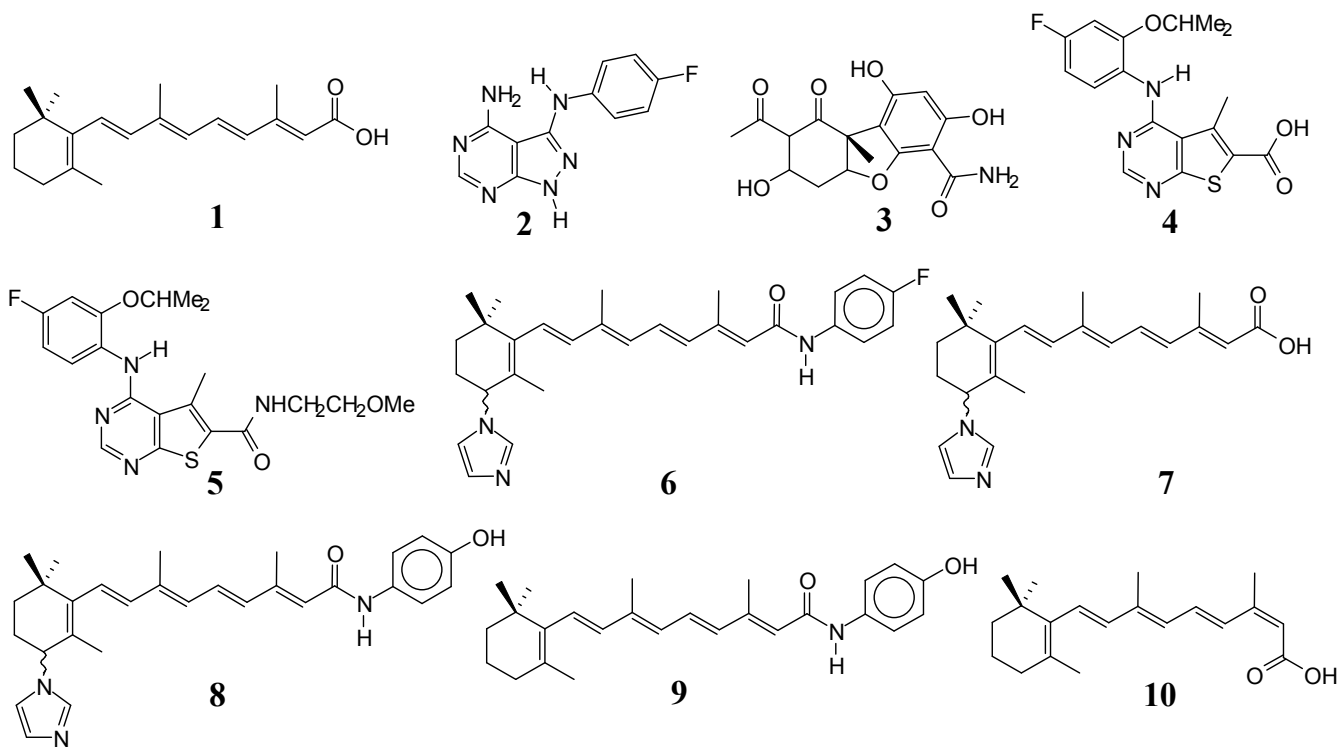

Figure 1: Chemical structures of compounds 1 – 10.

RESULTS AND DISCUSSIONS

Design Strategy: Rationale structural modifications of small molecules allow for their interactions with molecular target(s) in ways that could lead to improved drug-like compounds and possibly enhanced *in vivo* pharmacokinetic profiles.[13] Because of our desire to discover more efficacious anti-cancer agents, we were eager to exploit compound **10**'s scaffold as a strategy to novel potent/efficacious MNKDAs with improved drug-like properties. The rationale of using this scaffold is based on experimental and clinical reports that unlike ATRA (**1**), 13-CRA (**10**) has long elimination half-life in humans[14] and most animal species.[15] In addition, we also explored rational modification of the terminal amide moiety, C-4 heterocycles and the cyclohexene ring (**Figure 2**). It is relevant to state here that our previous studies with the ATRA

scaffold MNKDAs identified the C-4 azolyl retinamides to be superior to the corresponding carboxylic acid and esters.[8]

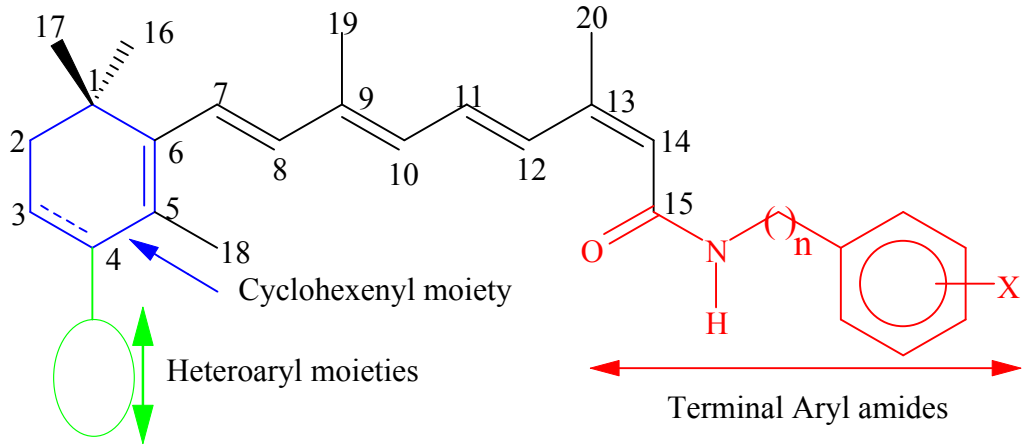

Figure 2: Overall Design Strategy for Novel C-4 Heteroaryl 13-Cis Retinamides

C-4 Azoyl/terminal Amide Modifications: Based on the continued successes of the C-imidazole retinamides with the ATRA scaffolds as promising anti-cancer agents,[8] we designed and synthesized compounds **16 - 25** as outlined in **Scheme 1**.

Cyclohexene Rigidification/C-4 Aryl and Heteroaryl Modifications: On the basis of previous studies which showed that structural rigidification that introduces conformational constrains around rotatable bonds contributed to higher specificity and potency, greater metabolic stability, and improved bioavailability,[16] we designed and synthesized several cyclohexadiene C-4 aryl substituted retinamides, compounds **33 - 40** (**Scheme 2**). A potential advantage of this strategy is that the achiral nature of these compounds would not require the tedious characterization of the racemates and pure enantiomers as would be required in advanced preclinical development for the chiral compounds of **Scheme 1**.[17]

Chemistry: Herein, we report, for the first time, the synthesis of **18** novel compounds based on the structural scaffold of 13-CRA (**10**), as outlined in **Schemes 1** and **2**.

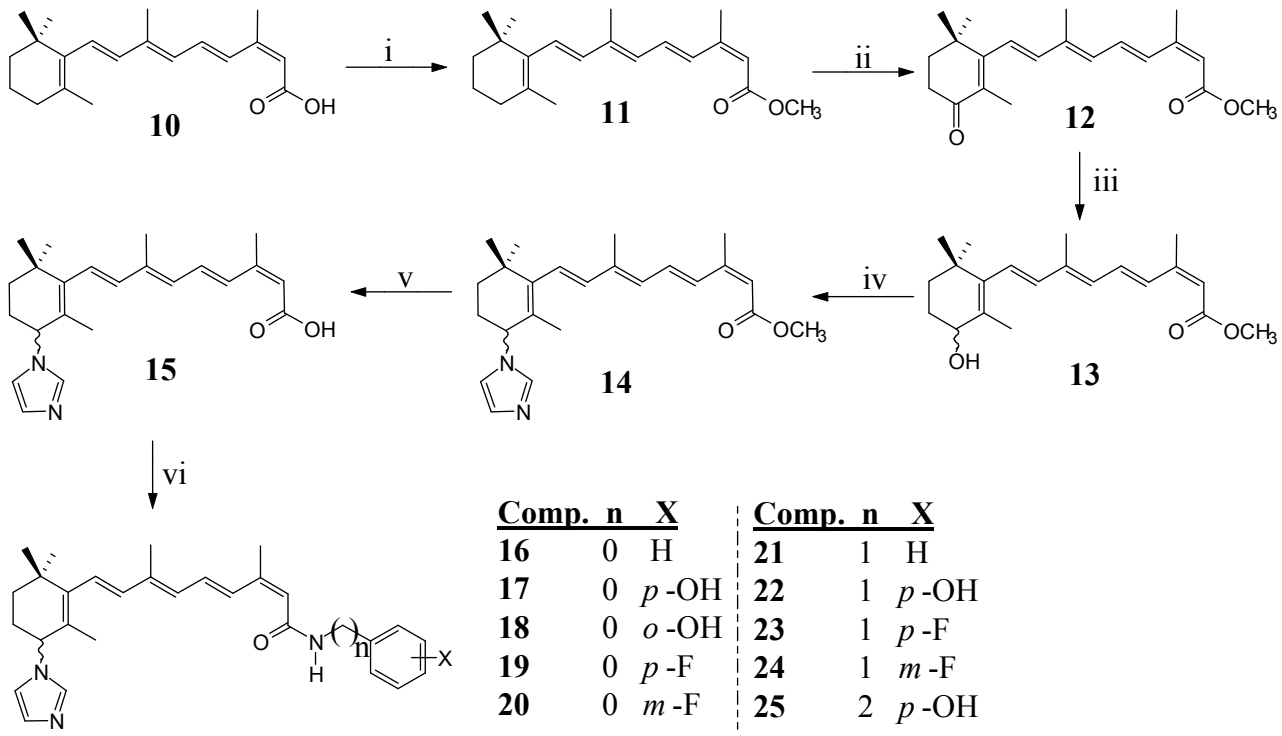

Comp.	n	X	Comp.	n	X
16	0	H	**21**	1	H
17	0	*p* -OH	**22**	1	*p* -OH
18	0	*o* -OH	**23**	1	*p* -F
19	0	*p* -F	**24**	1	*m* -F
20	0	*m* -F	**25**	2	*p* -OH

Scheme 1: Synthesis of C-4 Azoyl/terminal Amide Compounds 17 – 22[a]

[a]***Reagents and conditions:*** (i) $(CH_3)_3SiCHN_2$, MeOH/benzene; (ii) MnO_2, CH_2Cl_2; (iii) $NaBH_4$, MeOH; (iv) CDI, CH_3CN; (v) 2M KOH, MeOH, reflux; (vi) EDC, HOBT, DIEA, appropriate anilines, DMF.

The synthesis of (2*Z*,4*E*,6*E*,8*E*)-9-(3-(1*H*-imidazol-1-yl)-2,6,6-trimethylcyclohex-1-en-1-yl)-3,7-dimethylnona-2,4,6,8-tetraenoic acid (**15**) was carried out in five steps from the commercially available 13-CRA (**10**) and the procedure was adopted from our reported procedures of ATRA based retinamides.[12b] Protection of the carboxylic acid as the methyl ester (**11**) was done using trimethylsilyldiazomethane in hexanes followed by allylic oxidation using MnO_2 to give 4-oxo intermediate (**12**). Reduction of **12** using $NaBH_4$ gave the (±)-4-hydroxymethylterionate (**13**) which was further treated with carbonyldiimidazole (CDI) at ambient temperature to yield (±)-(1*H*-imidazol-1-yl)methylterionate (**14**). Alkaline hydrolysis of

14 in refluxing methanol gave the desired free acid **15** in 63% yield. Coupling of the respective amines with **15** was successfully achieved using ethyl(dimethylaminopropyl) carbodiimide (EDC), hydroxybenzotriazole (HOBt), diisopropylethylamine (DIEA) to give compounds **16** - **25** (**Scheme 1**), respectively, in average yields of ~50%.

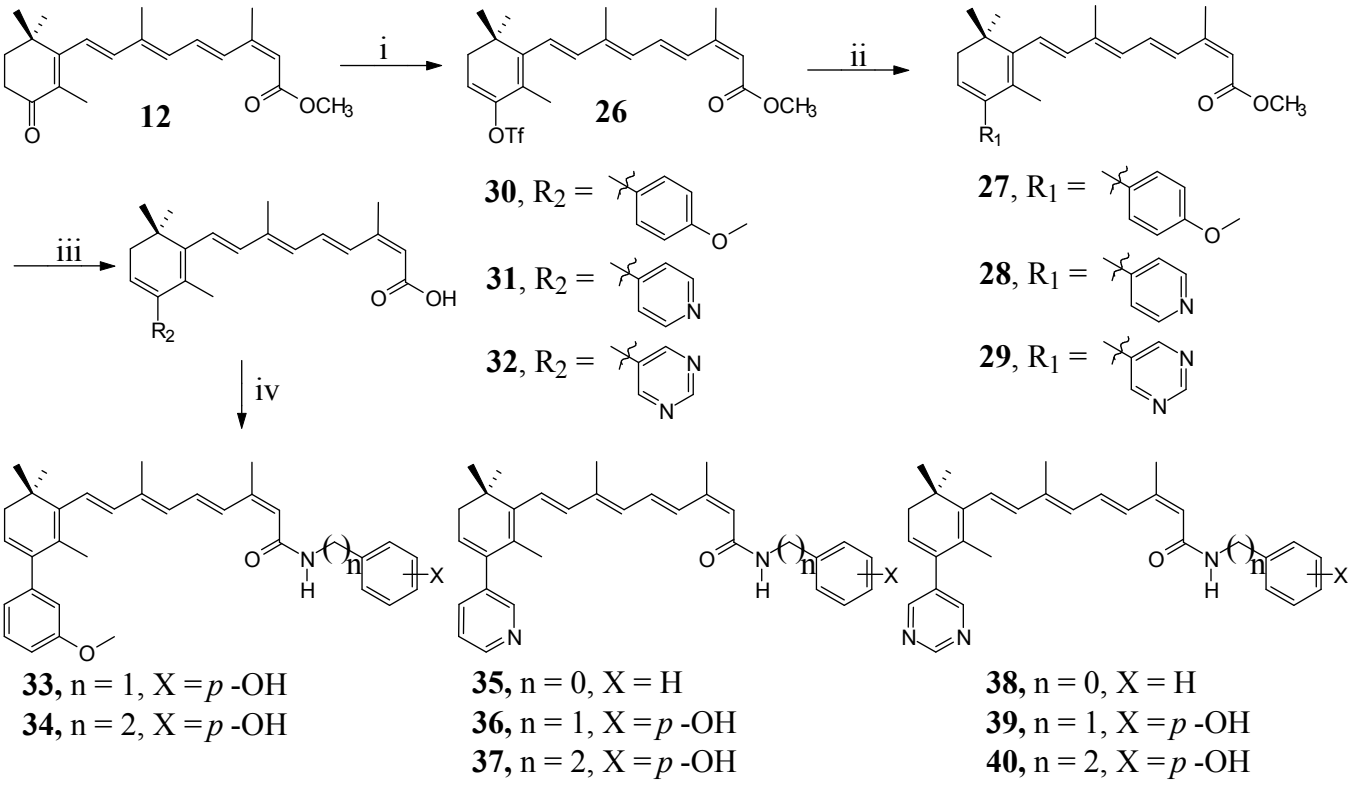

Scheme 2: Synthesis of Cyclohexen Rigidification/C-4 Aryl and Heteroaryl Retinamides[a]

[a]**Reagents and conditions:** (i) 5-Chloro-2-pyridyl triflimide, $NaN(SiMe_3)_2$, THF; (ii) 3-methoxybenzylboronic acid, $Pd(PPh_3)_4$, $CeCO_3$, dioxane, reflux; (iii) 2M KOH, MeOH, reflux (iv) EDC, HOBT, DIEA, appropriate benzylamine, DMF.

The synthesis of achiral C-4 aryl retinamides **33**-**40** (**Scheme 2**) commenced from the 4-oxo intermediate (**12)**. Generation of enolate using sodium bis(trimethylsilyl)amide in THF solution and trapping of the enolate with N-(5-chloro-2-pyridyl)bistrifluoromethanesulfonimide

furnished the vinyl triflate **26** in 75 % yield according to the reported procedure.[18] However, it should be noted that this reaction was carried out at -78°C throughout the reaction time, because, at higher temperatures, decomposition occurred and ≤ 20% of the products were obtained. Regiospecific palladium-catalyzed cross-coupling reaction with boronic acids[19] provided compounds **27- 29** in 88, 69 and 60% yields, respectively. Ester hydrolysis using 2M KOH gave the corresponding free acids **30 - 32** in 62, 48 and 70% yields, respectively. Coupling of these respective acids with appropriate amines was successfully achieved using EDC, HOBt and DIEA to give compounds **33 – 40**, respectively, in average yields of ~50% (**Scheme 2**).

Biological Studies:

Effects of 13-Cis retinamides on the Growth of Breast and Prostate Cancers Cells *in Vitro*. We determined the effects of the 13-cis NRs on human cancer cell proliferation using a variety of breast and prostate cancer cells lines using our previously described MTT assay procedures.[8, 12b, 20] The results (GI_{50} values) are summarized in **Table 1**. Growth inhibitory concentrations (GI_{50} values) are the concentrations of compounds that cause 50% growth inhibition obtained from dose-response curves. The clinically relevant retinoids, ATRA and 4-HPR and the Mnk inhibitor, cercosporamide were used as comparators in the assays.

Anti-proliferative activities in breast cancer cell lines: As stated earlier, the structural modification focused on modifications of the terminal amide, cyclohexe ring and C-4 substituents. As presented in **Table 1**, several important generalizations emerge from the anti-proliferative data. First, most of our compounds, including compounds **16** – **25**, possess higher

anti-proliferative activities towards all four breast cancer cell lines than the positive controls, ATRA, 4-HPR and the Mnk inhibitors, as evidenced by the lower GI_{50} values (**Table 1**).

Table 1: Inhibitory concentrations (GI_{50}, µM) of NRs and reference compounds on the Growth of Human Breast Cancer Cells *in Vitro*

Cpds.	GI_{50}s (µM) MCF-7	GI_{50}s (µM) MDA-MB-231	GI_{50}s (µM) MDA-MB-468	GI_{50}s (µM) SKBR-3
16	1.90 ± 0.00	1.74 ± 0.22	2.54 ± 0.12	1.73 ± 0.09
17	1.99 ± 0.26	13.05 ± 1.06	6.83 ± 0.33	3.89 ± 0.12
18	1.09 ± 0.00	4.67 ± 0.14	3.03 ± 0,39	3.89 ± 0.06
19	0.40 ± 0.08	4.95 ± 0.24	4.57 ± 0.00	25.11 ± 1.03
20	5.49 ± 0.11	8.51 ± 0.16	6.76 ± 0.23	16.98 ± 0.79
21	9.77 ± 0.64	5.88 ± 0.27	7.24 ± 0.14	10.71 ± 0.98
22	0.16 ± 0.00	2.23 ± 0.07	2.70 ± 0.35	2.45 ± 0.09
23	1.93 ± 0.16	1.41 ± 0.06	2.45 ± 0.06	5.50 ± 0.00
24	1.81± 0.15	1.65 ± 0.04	3.09 ± 0.18	4.24 ± 0.21
25	1.90 ± 0.08	2.88 ± 0.08	13.48 ± 0.97	1.41 ± 0.03
33	*	*	*	*
34	*	*	*	*
35	8.32 ±	25.11 ± 0.76	39.81 ± 1.33	47.40 ±
36	*	*	*	*
37	8.75 ±	26.91 ± 0.98	50.11 ± 2.40	42.24 ±
38	7.01 ±	26.91 ± 1.23	22.90 ± 1.03	30.98 ±

39	4.96 ±	11.48 ± 1.07	19.05 ± 1.22	11.48 ±
40	2.96 ±	14.45 ± 0.92	23.44 ± 0.96	23.99 ±
ATRA[b]		14.12 ± 0.86	14.12 ± 0.55	22.90 ± 0.15
4-HPR	4.65 ±	11.05 ±	6.02 ±	3.98 ±
Cerco.[b]		43.65 ± 0.17	47.86 ± 0.23	26.02 ± 0.87

[a] The GI_{50} were determined from dose-response curves (by nonlinear regression analysis using GraphPad Prism) compiled from at least three independent experiments using indicated breast cancer cells, SEM < 10%, and represents the compound concentration required to inhibit cell growth by 50%.

[b] Previously reported in Ramalingam S, *et al*.[8a] * represents ≥ 60% inhibition of breast cancer cell growth at 10 μM.

Second, for each compound, the anti-proliferative activities towards the breast cancer cell lines varied significantly. In general, the MCF-7 cell line was the most sensitive, while the SKBR-3 were the least sensitive to these compounds. Third, for a given breast cancer cell line, the anti-proliferative activity depends largely on the structure of the NR, which in turn depends largely on the nature of the C-4 heterocycle and cyclohexen/cyclohexadiene ring. [1] Compounds with the imidazole tethered to C-4 of the cyclohexene ring (**16** – **25**) exhibit more potent anti-proliferative activities than compounds with phenyl (**33** and **34**), pyridine (**35** – **37**) or pyrimidine (**38** – **40**) tethered to C-4 of the cyclohexadiene ring. [2] Compared to compound **16** which possess an unsubstituted amide phenyl ring, compounds with substituted hydroxyl (**17** and **18**) or fluoro (**19** and **20**) groups displayed mixed anti-proliferative activities, but in general were either

equipotent or less active than compound **16**. The only exception was *p*-fluoro compound (**19**) with a GI_{50} = 0.4 μM against MCF-7 cells was ~4.8 fold more potent than **16** (GI_{50} = 1.90 μM). [3] Insertion of a methylene moiety between the amide and phenyl group clearly led to decreased anti-proliferative activities (compare GI_{50}s of **16**: 1.74 – 2.54 μM to GI_{50}s of **21**: 5.88 – 10.71 μM). [4] However, ortho/para hydroxyl or fluoro substitutions to benzyl group of **21** to give compounds **22** – **24** led to enhanced anti-proliferative activities across the four breast cancer cell lines. Amongst these three compounds, **22** was the most potent with GI_{50} values of 0.16, 2.23, 2.70 and 2.45 μM *versus* MCF-7, MDA-MB-231, MDA-MB-468 and SKBR-3 cell lines, respectively. Related compound **25** with an ethylene moiety between the amide and *p*-hydroxyl group led to varied anti-proliferative activities. It is notable that **25** amongst these compounds, exhibited the best activity (GI_{50} = 1.41 μM) against SKBR-3 cell line.

Anti-proliferative activities in prostate cancer cell lines: The GI_{50} values of compounds **16** – **22** against three human prostate cancer cell lines, including, LNCaP, CWR22Rv1 and PC-3 were determined and compared to the GI_{50} values of clinically relevant drugs, ATRA, 4-HPR, casodex and MDV3100 (enzalutamide) (**Table 2**). In general, the compounds were more potent than ATRA, but were equipotent to 4-HPR, casodex and MDV3100. The PC-3 cell line was the least sensitive to all the compounds tested. Compounds **20** and **22** exhibited the most potent anti-proliferative activities across the three cell lines.

Table 2: Inhibitory concentrations (GI_{50}, µM) of NRs and reference compounds on the Growth of Human Prostate Cancer Cells *in Vitro*

Cpds.	GI_{50}s (µM)[a] LNCaP	GI_{50}s (µM)[a] CWR22Rv1	GI_{50}s (µM)[a] PC-3
16	2.69 ± 0.09	1.28 ± 0.03	8.91 ± 0.51
17	3.54 ± 0.18	3.89 ± 0.08	11.74 ± 0.76
18	3.23 ± 0.19	2.23 ± 0.11	15.48 ± 0.87
19	3.89 ± 0.23	8.12 ± 0.52	30.19 ± 0.94
20	2.69 ± 0.14	2.04 ± 0.01	5.62 ± 0.03
21	*	*	*
22	1.69 ± 0.07	1.86 ± 0.06	3.54 ± 0.02
ATRA[b]	47.86 ± 0.21	25.11 ± 0.16	36.3 ± 0.27
4-HPR[b]	2.69 ± 0.14	3.23 ± 0.08	3.54 ± 0.09
Casodex[b]	2.61 ± 0.09	3.81 ± 0.18	9.15 ± 0.14
MDV3100[b]	2.88 ± 0.13	3.34 ± 0.25	9.15 ± 0.26

[a] The GI_{50} were determined from dose-response curves (by nonlinear regression analysis using GraphPad Prism) compiled from at least three independent experiments using LNCaP cells, SEM < 10%, and represents the compound concentration required to inhibit cell growth by 50%.

[b] Previously reported in Ramamurthy V *et al.*[8b] * Indicates compound requirement > 100 µM to induce 50 % inhibition of cell growth in PC cells

***In vitro* characterization of compounds 16, 20 and 22 in breast cancer cell lines:** We previously reported that the anti-proliferative effects of the 1st generation MNKDAs in breast cancer cells was due to degradation of Mnk1/2 with subsequent depletion of peIF4E and induction of apoptosis.[8a] To determine if these compounds modulate Mnk1/2 and related oncogenic proteins, we performed western blot of lysates from MCF-7, MDA-MB-231 and MDA-MB-468 human breast cancer cells treated with compounds **16**, **20**, and **22** or with vehicle (DMSO, negative control) or compound **6** (positive control). **Figure 3A-C** shows that the three compounds significantly and dose-dependently, reduced the expressions of Mnk1, Mnk2 and peIF4E, with no noticeable effects on the expression of total eIF4E. The compounds also caused dose-dependent formation of c-PARP which indicates induction of cell death (apoptosis).

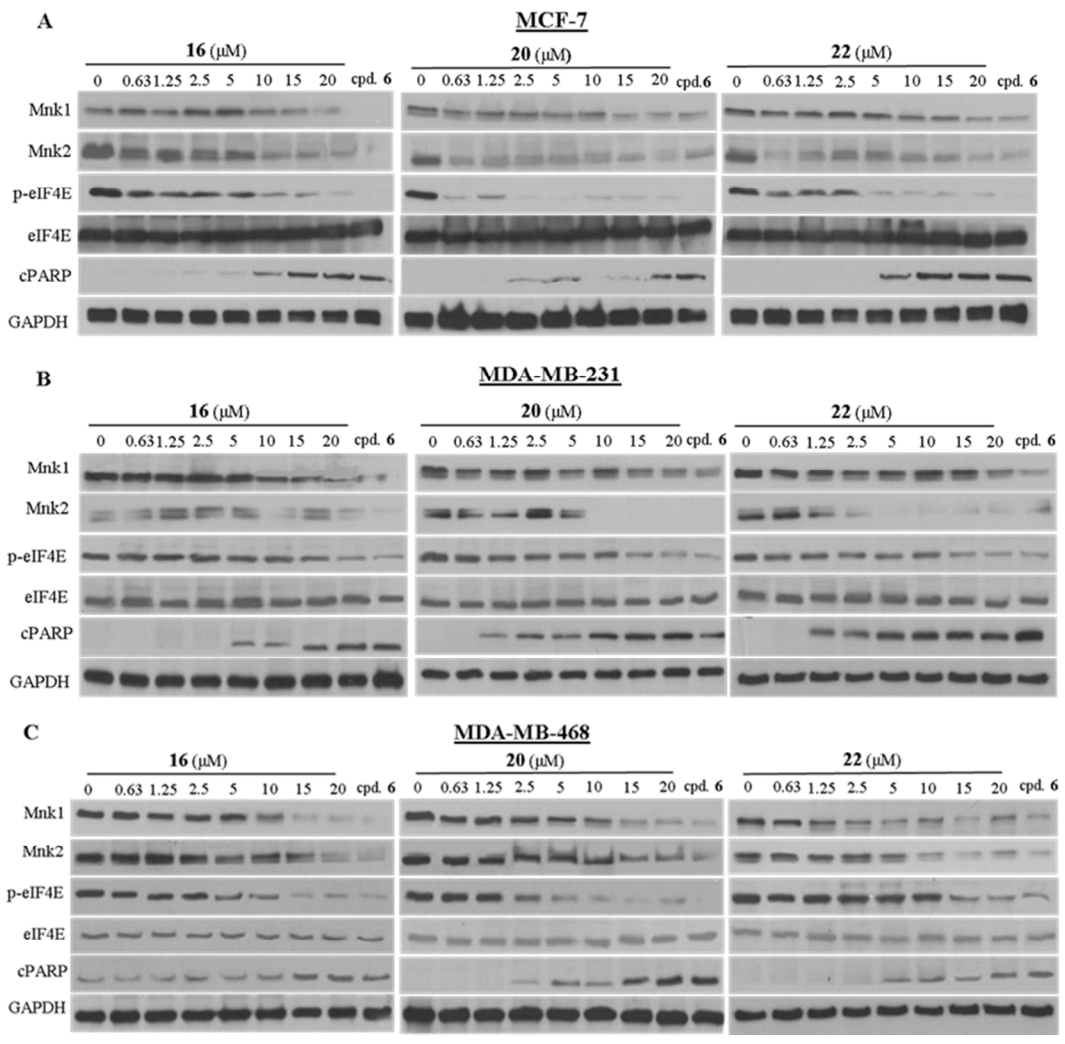

Figure 3: Effect of compounds 16, 20 and 22 on Mnk1 and 2, peIF4E, eIF4E and cPARP proteins in MCF-7 cells. Equal protein concentrations from MCF-7 (**A**), MDA-MB-231 (**B**) and MDA-MB-468 (**C**) cells treated for 24 h with **16, 20** and **22** at the various concentrations as indicated and **6** (20 μmol/L) were separated by SDS-PAGE and western blots probed with antibodies to Mnk1 and 2, peIF4E, eIF4E and cPARP. Vehicle treated cells were included as control and all blots were reprobed for GAPDH for loading control.

Based on previous studies with closely related compound,[8] we evaluated the inhibitory effects of compounds **16**, **20** and **22** on cell migration, using the human metastatic breast cancer cell line, MDA-MB-231 by wound-healing assay. **Figure 4** shows that the compounds **20** and **22** significantly inhibited migration of MDA-MB-231 cells compared to the control. At 24 h after cell monolayers were wounded, control cells had completely filled in the scratched area.

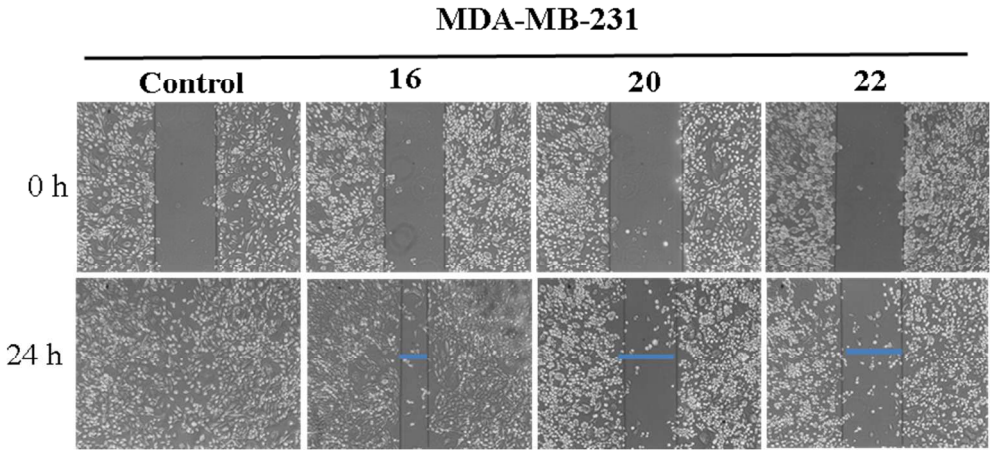

Figure 4: Effects of compounds 16, 20 and 22 on MDA-MB-231 cell migration: MDA-MB-231 cells (5 x 10^5 cells/well) were seeded on Boyden chamber, grown to confluence and scratches made at experimental time zero. The cells were treated with indicated compounds (5 μM each) for 24h. Representative photomicrographs of initial and final wounds are shown at 100x magnification.

***In vitro* characterization of compounds 16, 20 and 22 in prostate cancer cell lines:** Previously, we demonstrated that the anti-tumor activity of the early NRs in prostate cancer cells was due to simultaneous inhibition of the Mnk/eIF4E and androgen receptor (AR) signaling pathways.[8b] Similar to studies described above, we performed western blot of lysates from LNCaP human prostate cancer cells treated with compounds **16**, **20**, and **22** or with vehicle (DMSO, negative control). **Figure 5A** shows that the three compounds significantly and in a dose-dependent fashion, reduced the expressions of fAR, Mnk1 and Mnk2, with no noticeable effects on the expression of total eIF4E. In addition, the compounds caused significant depletion of oncogenic cyclin D1 and they each induced cleaved PARP (c-PARP), a reliable marker of apoptotic cell death (**Figure 5B**).

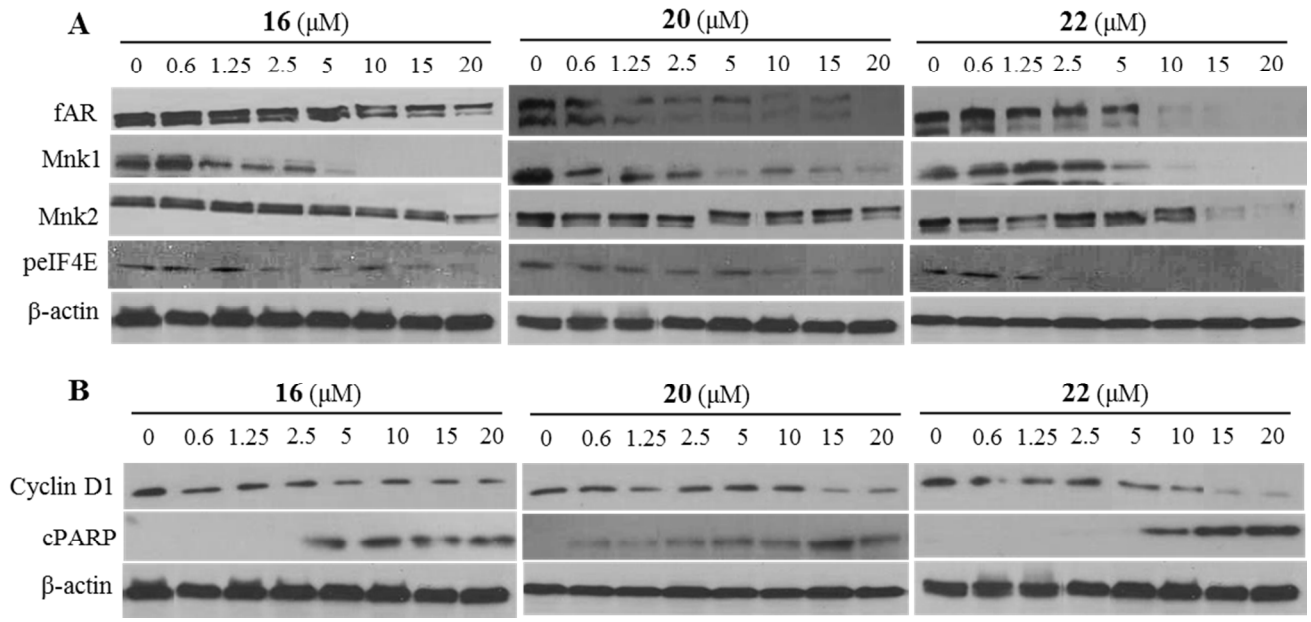

Figure 5: Effects of compounds 16, 20 and 22 on the expression of fAR, Mnk, peIF4E, cyclin D1 and cleaved PARP in LNCaP cells. Equal protein concentrations from LNCaP cells treated with **16, 20 and 22** at different concentrations (0.6-20 μM) for 24 h were separated by SDS-PAGE and western blots probed with antibodies to fAR, Mnk1/2, peIF4E, cyclin D1 and

cleaved PARP. Vehicle treated cells were included as a control and all blots were reprobed for β-actin for loading control.

Based on previous studies with closely related compound,[8] we evaluated the inhibitory effects of compounds **16**, **20** and **22** on cell migration, using the human metastatic PC cell line, PC-3 by wound-healing assay. **Figure 6** shows that the three compounds significantly inhibited migration of PC-3 cells compared to the control. At 24 h after cell monolayers were wounded, control cells had completely filled in the scratched area.

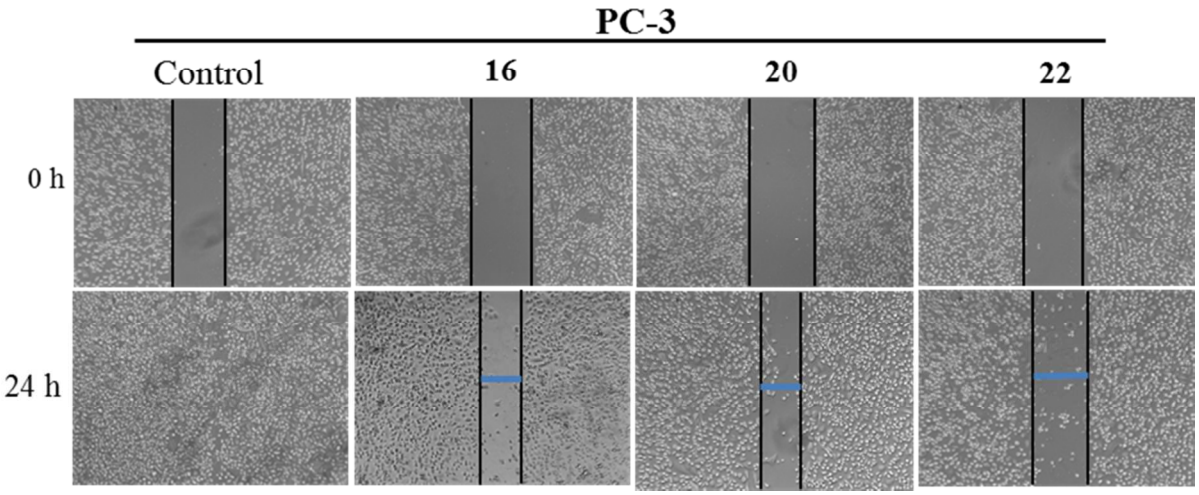

Figure 6: Effects of compounds 16, 20 and 22 on PC-3 cell migration: PC-3 cells (5 x 10^5 cells/well) were seeded on Boyden chamber, grown to confluence and scratches made at experimental time zero. The cells were treated with indicated compounds (5 μM each) for 24h. Representative photomicrographs of initial and final wounds are shown at 100x magnification.

Since AR is a major driver of proliferation in PCa,[21] we next examined the effect of these three compounds on AR transcriptional activity in LNCaP cells. As shown in **Figure 7,** 24 h exposure of LNCaP cells to lead NRs, **16**, **20**, and **22** (10 μM) resulted in a 2 – 4-fold dramatic

inhibition of DHT induced AR transcriptional activity that was however less potent than that observed upon clinically available MDV3100 treatment. Of these leads, compound **20** was the most potent.

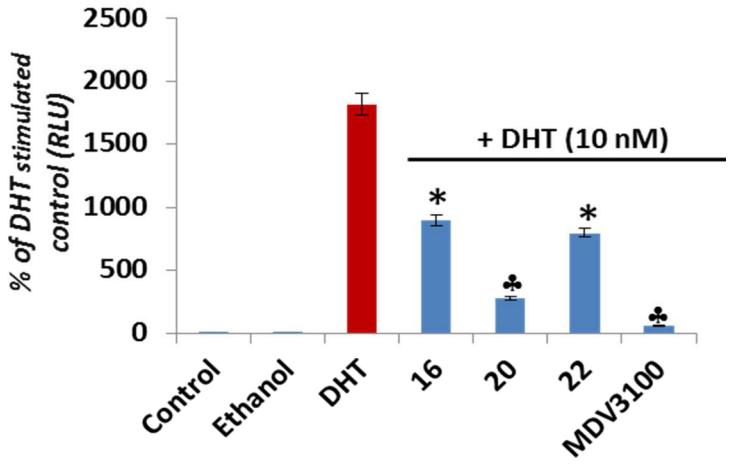

Figure 7: Effects of compounds 16, 20, and 22 on DHT-induced AR transactivation in LNCaP cells. LNCaP cells dual transfected with ARR2-Luc and the *Renilla* luciferase reporting vector pRL-null and treated with 10 μM of specified compounds for 18 h in the presence of 10 nmol/L dihydrotestosterone (DHT). Control represents baseline activity without androgen stimulation. Androgen stimulated luciferase activity (luminescence) was measured in a victor 1420 plate reader. The results are presented as the fold induction (i.e., the relative luciferase activity of the treated cells divided by that of control) normalized to that of *Renilla*. *, $P< 0.05$; ♣, $P<0.01$ compared with DHT alone treated cells.

To confirm whether AR and Mnk1 are the major anti-cancer targets of these compounds on LNCaP cells, we analyzed the percentage of cell survival in LNCaP cells by MTT assay following transient transfection with AR siRNA and/or Mnk1 siRNA for 18h. Here, we present data for compound **20** which are identical to data for compounds **16** and **22**. The efficiency of

transfection was confirmed by western blot analysis, wherein protein lysates obtained from the transfected cells after AR siRNA transfection showed a temporal decrease in total AR protein and cells transfected with Mnk1 siRNA showed a temporal decrease in the expression Mnk1 compared to scrambled (si-control) treated controls after 18 h of transfection (**Figure 8A**). Cells co-treated with AR and Mnk1 siRNA showed a remarkable decrease in the expression of both AR and Mnk1 compared to scrambled siRNA treated cells (**Figure 8A**). MTT assay revealed that transient transfections with AR and/or Mnk1 siRNA caused a considerable decrease (~ 40%) in LNCaP cell viability compared to control (**Figure 8B**, compare lane 1 to lanes 4, 7 and 10). Treatment of LNCaP cells (*un-transfected*) with 5 μM concentration of compound **20** for 72 h showed a robust reduction in cell viability (lane 3). LNCaP cells harboring AR (lane 6) or Mnk1 (lane 9) knockdown also displayed a significant decrease in cell viability upon treatment with 5 μM of compound **20**, compared to the Mnk1 and AR siRNA alone treated counterparts (lanes 4 and 7, respectively). However, LNCaP cells with double knockdown of AR and Mnk1 genes (lane 12) did not show any significant decrease in cell viability upon agent treatment compared to cells co-treated with Mnk1 and AR siRNA (**Figure 8B**, lane 10). These results strongly suggest that Mnk1 and AR are prime targets of compounds **16**, **20** and **22**, and that loss of both these targets abolishes the potent growth-inhibitory effects mediated by these agents in LNCaP cells.

We note that although siRNA knockdown and treatment with compound **20** is expected to cause a similar percent of decrease in cell viability, the effect of siRNA on LNCaP cell proliferation depends on the treatment period and dose of siRNA used for transfection. In our study, we have transfected LNCaP with 100 nM of AR/MNK1 siRNA for 18 h. siRNA transfection for 18-24 h typically results in only 30% of drop in cell viability.[22] Only in cases

where transfections are carried out for up to 96 h do massive drop in cell proliferation of ~12-15% (i.e., 85-88% growth inhibition) occur.[23] Furthermore, the mechanisms by which AR/MNK siRNA and compound **20** act are different. Whereas siRNA works at the level of transcription, compound **20** acts at the post-translational level and hence even though compound **20** recapitulates AR/MNK siRNA affects, the percentage of decrease in cell proliferation caused by the two agents (i.e., siRNA and NRs) are not alike.

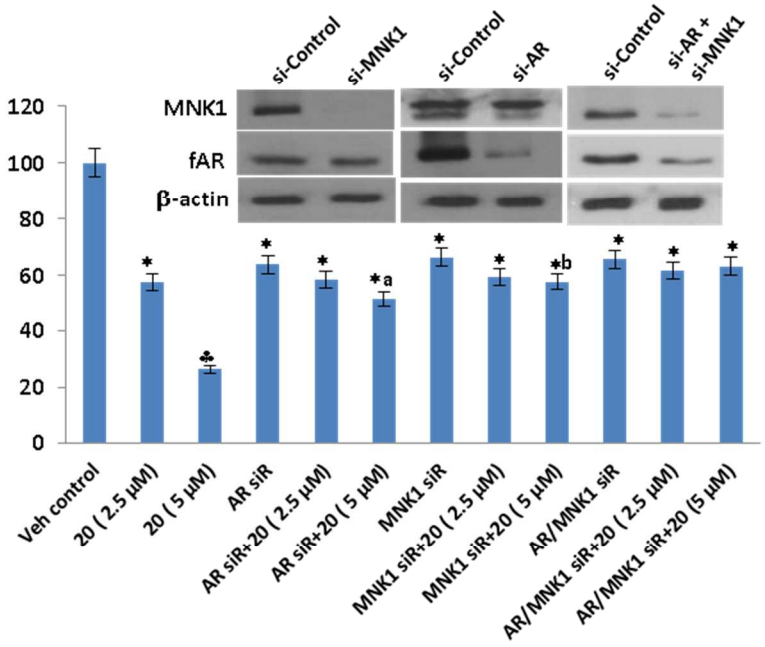

Figure 8: Effects of NRs on the viability of LNCaP cells transiently knocked-down for AR and/or Mnk1. (**A**) Western blot analysis of the expression of fAR and Mnk1 in LNCaP cells transfected with 100 nM of siAR, siMnk1 and combinations for 18 h. (**B**) Effect of compound 20 (in μM concentration) on cell proliferation in LNCaP cells transfected with 100 nM of siAR, siMNK1 and combinations as determined by MTT assay. The results represent the mean ± SEM of three independent experiments and are represented as a bar graph after normalizing to control cells. *, $P< 0.05$; ♣, $P<0.01$ compared with vehicle treated control; a- Significantly different

from AR siR treated cells, $P< 0.05$; b- Significantly different from MNK1 siR treated cells, $P< 0.05$.

Inhibition of breast and prostate cancer tumor growth *in vivo*: To determine whether the anti-cancer effects exhibited by the lead compounds in cell cultures could be replicated in animal models, we conducted anti-tumor xenograft studies in two well-established aggressive models of human breast (MDA-MB-231) and prostate (CWR22Rv1) cancers. As noted above, although compounds **16**, **20** and **22** are equipotent, we selected the latter two compounds for *in vivo* studies based on their ease of synthesis, availability and animal cost.

MDA-MB-231 anti-tumor efficacy study: First, we evaluated the *in vivo* antitumor efficacy of compounds **20** and **22** in mice bearing MDA-MB-231 triple negative breast cancer (TNBC) xenografts that were administered intraperitoneal (i.p.) 20 mg/kg compound **20** or **22** 5x/week over 28 days, which resulted in an 85.4% suppression of tumor growth. Indeed, the two compounds were equipotent (**Figure 9A**). Thus, the tumor growth inhibition, measured as %T/C = 14.6%, classified these compounds as highly efficacious according to the National Cancer Institutes (NCI'S) criteria.[24] Tumor growth inhibition (%T/C), is defined as the ratio of the median tumor volume for the treated *versus* control group. Representative photos of the tumor-bearing mice in the control and the two treatment groups at termination of experiment (day 28) are presented in **Figure 9B**. Importantly, the mice in the treated group did not lose body weight (**Figure 9C**) and display any signs of toxicity, suggesting no apparent adverse events of the compounds.

For the sake of comparison, with our early lead, compound **6** (based on ATRA scaffold)[8] caused 97% suppression of MDA-MB-231 tumor growth (data not shown).[25] These data suggest that compounds **20** and **22** can be classified as *strong back-up compound*s in our novel retinamides drug discovery and development program. It is important to state here that addition anti-tumor studies are need in several breast cancer models in addition to rigorous pharmacokinetics/pharmacodynamics and toxicology studies to identify the compound that will emerge as our Investigation New Drug (IND) candidate. It is also pertinent to note that our current clinical agent, galeterone that emerged from our prostate cancer drug discovery program was a back-up compound at the early stage of the development process.[26] Galeterone has successfully completed phase II clinical trials in castration resistant prostate cancer (CRPC) patients and is scheduled to enter pivotal phase III clinical trials in the 1st half of this year.[26]

Molecular analysis of tumors: To assess their *in vivo* mode of action, we evaluated the effects of compounds **20** and **22** on Mnk-1, peIF4E and their downstream targets. As expected, tumors from mice treated with compounds **20** or 22 showed depletion of Mnk1/2, peIF4E, cyclide D1 and anti-apoptotic Breast cancerl-2 with concomitant up-regulation of pro-apoptotic proteins, Bad and Bax (**Figure 9D**).

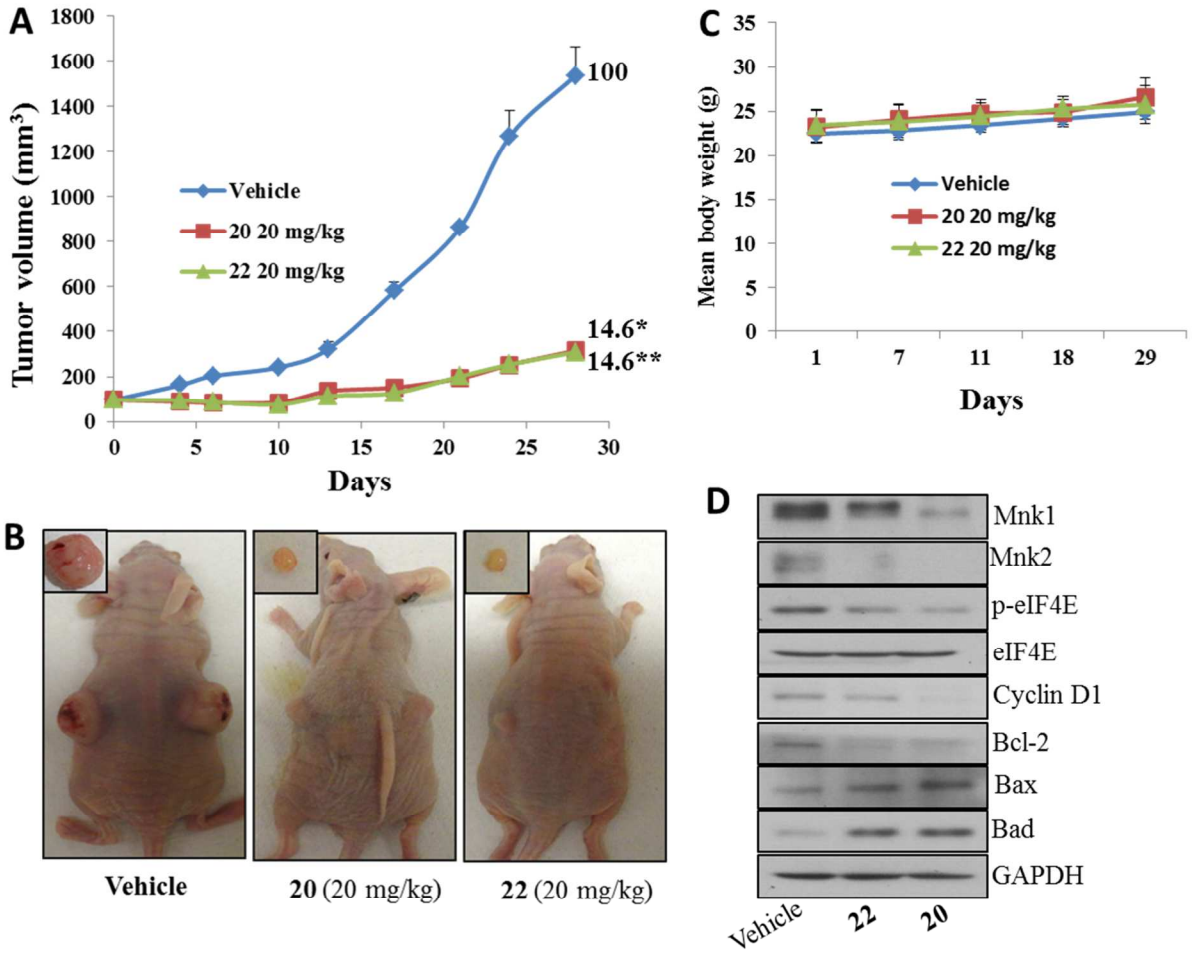

Figure 9: Compounds 20 and 22 suppress breast xenograft tumor growth *in vivo*. (**A**) Nude female mice bearing MDA-MB-231 xenograft tumors (n = 6/group) were treated with **20** or **22**, administered i.p. 20 mg/kg/day, 5 days per week for 28 days. %T/C values are indicated to the right of each growth curve and the error bars are the SEM. Compounds **20** and **22** treatments, each, significantly suppressed tumor growth (for **20**, *, $p = 0.0001$ and for **22**, **, $p = 0.0001$). (**B**) Representative photos of the tumor-bearing mice and excised tumors in the control and the two treatment groups at termination of experiment (day 28). (**C**) Body weight changes of the mice during the course of treatments. Animals were monitored for changes in body weight as a surrogate marker for toxicity in control and treatment groups. (**D**) The effect of compounds on

the expression of proteins modulated by Mnk/eIF4E signaling. Total cell lysates in mice treated with vehicle, compound 20 and 22 were prepared separately using RIPA buffer. Total protein (50µg/well) from pooled samples (n=6) was run on 10% SDS-PAGE and probed with antibodies for MNK1, MNK2, p-eIF4E, eIF4E, cyclin D1, Breast cancerl-2, Bax, Bad and GAPDH.

CWR22Rv1 anti-tumor efficacy study: Similarly, treatment of compound **20** to castrated mice bearing the aggressive CWR22Rv1 xenografts cause significant inhibition of tumor growth with % T/C value of 38.8, i.e., 61.2% suppression of tumor growth (**Figure 10A**). We also found that the body weights were comparable in mice either from vehicle control or treatment groups (**Figure 10B**), suggesting no apparent adverse effects of compound **20**.

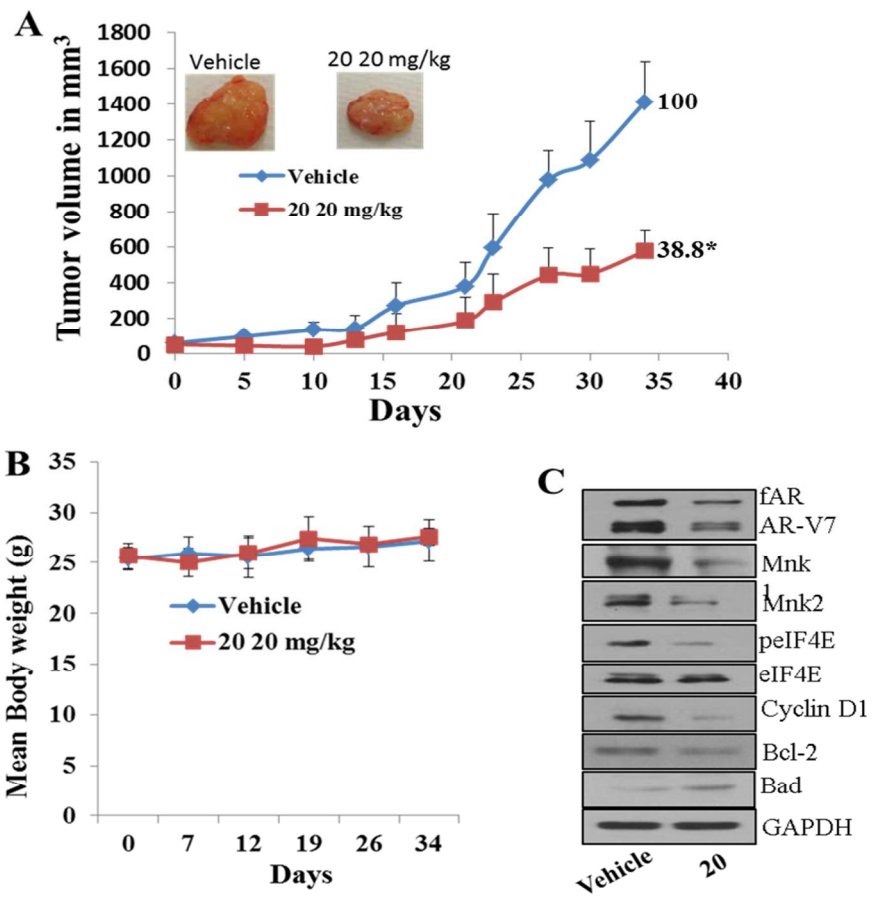

Figure 10: Compound 20 suppresses prostate xenograft tumor growth *in vivo*. (**A**) Castrated SCID male mice bearing CWR22Rv1 xenograft tumors (n = 6/group) were treated with **20**, administered i.p. 20 mg/kg/day, 5 days per week for 28 days. %T/C values are indicated to the right of each growth curve and the error bars are the SEM. Compounds **20** treatment significantly suppressed tumor growth (***** $p = 0.0001$). (**B**) Body weight changes of the mice during the course of treatments. Animals were monitored for changes in body weight as a surrogate marker for toxicity in control and treatment groups. (**C**) The effect of compounds on the expression of proteins modulated by AR and Mnk/eIF4E signaling. Total cell lysates in mice treated with vehicle, compound 20 and 22 were prepared separately using RIPA buffer. Total protein (50µg/well) from pooled samples (n=6) was run on 10% SDS-PAGE and probed with antibodies for fAR, AR-V7, MNK1, MNK2, p-eIF4E, eIF4E, cyclin D1, Breast cancerl-2, Bad and GAPDH.

Molecular analysis of tumors: To assess their *in vivo* mode of action, we evaluated the effects of compounds **20** on fAR, AR-V7, Mnk-1, peIF4E and their downstream targets. As expected, tumors from mice treated with compounds **20** showed depletion of fAR, AR-V7, Mnk1/2, peIF4E, cyclin D1 and anti-apoptotic Breast cancerl-2 with concomitant up-regulation of pro-apoptotic proteins, Bad (**Figure 10C**).

CONCLUSIONS

Our study has shown for the first time that high anti-cancer activities can be retained in C-4 heteroaryl retinamides based on the rarely utilized 13-cis retinoic acid scaffold. In this study, we describe a series of novel C-4 heteroaryl 13-cis retinamides that degrade Mnk 1 and 2 with concomitant suppression of oncogenic eIF4E phosphorylation in a variety of human breast and

prostate cancer cell lines. In addition, the compounds also modulate activities of full-length and splice variant androgen receptors (fAR and AR-V7) via AR antagonism and AR degradation in prostate cancer cells. Three lead compounds, including **16**, **20** and **22** were identified. Of these compounds, **20** and **22** exhibited equipotent and strong suppression of the growth of aggressive human triple negative breast cancer MDA-MB-231 tumor xenografts. Compound **20** also proved to be very effective at inhibiting the growth of castration-resistant CWR22Rv1 human prostate tumor xenografts. These impressive *in vitro* and *in vivo* anti-breast and anti-prostate cancers activities make compounds **20** and **22** strong candidates for further development as potential new drugs for the treatments of breast and prostate cancers in humans. In addition, given the implication of Mnk1/2-eIFE axis in the initiation and progressions of all types of solid tumors[27] and hematologic cancers,[28] these and related retinamides warrant evaluation in other types of cancers.

EXPERIMENTAL SECTION

Chemistry: *General:* All the materials listed below were of research grade or spectrophotometric grade in the highest purity commercially available from Sigma-Aldrich. Column chromatography was performed on silica (230-400 mesh, 60 Å) from Silicycle. Silica gel plates (Merck F254) were used for thin layer chromatography (TLC) and were developed with mixtures of ethyl acetate (EtOAc)/Petroleum ether or CH_2Cl_2/methanol (MeOH) unless otherwise specified and were visualized with 254 and 365 nm light and I_2 or Br_2 vapor. Petroleum ether refers to light petroleum, bp 40-60 °C. ^1H and ^{13}C NMR spectra were recorded in $CDCl_3$ or DMSO-d_6 using a Brüker 400 MHz NMR instrument and chemical shifts are reported in ppm on the δ scale relative to tetramethylsilane. High resolution mass spectra were

obtained on Bruker 12 T APEX-Qe FTICR-MS instrument by positive ion ESI mode by Susan A. Hatcher, Facility Director, College of Sciences Major Instrumentation Cluster, Old Dominion University, Norfolk, VA. Melting points (mp) were determined with Fischer Johns melting point apparatus uncorrected. Purities of the compounds were determined by Waters UPLC BEH C18 1.7µl, 2.1×50mm column using a solvent gradient system of ammonium acetate buffer/acetonitrile/methanol (100→0, 0→100 and 0→10 respectively) over a period of 10 min. The purities of all final compounds were determined to be at least 95% pure by a combination of UPLC, NMR and HRMS.

(2*Z*,4*E*,6*E*,8*E*)-methyl 3,7-dimethyl-9-(2,6,6-trimethylcyclohex-1-en-1-yl)nona-2,4,6,8-tetraenoate (11)

In a 250 mL round bottomed flask (RBF) equipped with a magnetic stirrer, 13-*cis*-retionoic acid (**10**) (5 g, 16.64 mmol) was dissolved in methanol (30 mL) and benzene (100 mL). While stirring, trimethylsilyldiazomethane solution 2.0M in hexanes (3.730 g, 32.68 mmol) was added drop-wise very slowly and reaction was monitored by the gas evolution on the oil bubbler. The reaction mixture was concentrated to give an oily yellow crude product. Purification by flash column chromatography [FCC; petroleum ether/EtOAc (9:1)] afforded compound **11** as a yellow solid. Yield: 4.32 g (83%); mp: 38-40°C; ^{1}H NMR (400 MHz, $CDCl_3$) δ 7.77 (d, *J* = 15.3 Hz, 1H), 6.99 (dd, *J* = 15.3, 11.5 Hz, 1H), 6.32 – 6.21 (m, 2H), 6.15 (d, *J* = 16.1 Hz, 1H), 5.64 (s, 1H), 3.70 (s, 3H), 2.07 (s, 3H), 2.03 (t, *J* = 6.2 Hz, 2H), 1.99 (s, 3H), 1.71 (s, 3H), 1.65 – 1.54 (m, 2H), 1.47 (dd, *J* = 7.7, 3.9 Hz, 2H), 1.03 (s, 6H); ^{13}C NMR (100 MHz, $CDCl_3$) δ 166.8, 151.3, 139.8, 137.6, 137.4, 132.2, 130.3, 130.0, 129.2, 128.5, 128.3, 116.0, 77.3, 77.0, 76.7, 50.9, 39.6, 34.2, 33.1, 28.9, 21.7, 20.9, 19.2, 12.8.

(2*Z*,4*E*,6*E*,8*E*)-methyl 3,7-dimethyl-9-(2,6,6-trimethyl-3-oxocyclohex-1-en-1-yl)nona-2,4,6,8-tetraenoate (12)

In a 500 mL volumetric flask, **11** (4.00 g, 12.7 mmol), MnO_2 (100 g, 1150 mmol) were added into 100 mL of dichloromethane. The mixture was allowed to stir on an Innova 2000 platform shaker at 200 rpm for 12 h**.** Filtration was done through a pad of celite and the organic reaction mixture concentrated to give thick yellow oil. This was adsorbed on silica (50 g) and packed on a column where elution was done gravity with a solvent system of [petroleum ether/EtOAc (9:1)] to yield compound **12** as a yellow solid. Yield: 2.80 g (68%); mp: 83-85°C; ^{1}H NMR (400 MHz, $CDCl_3$) δ 7.85 (d, *J* = 15.4 Hz, 1H), 6.96 (dd, *J* = 15.3, 11.4 Hz, 1H), 6.35 (dd, *J* = 12.5, 7.6 Hz, 3H), 5.70 (s, 1H), 4.12 (q, *J* = 7.1 Hz, 2H), 3.71 (s, 3H), 2.51 (t, *J* = 6.8 Hz, 2H), 2.08 (s, 3H), 2.02 (s, 3H), 1.86 (s, 3H), 1.26 (t, 2H), 1.19 (s, 6H). ^{13}C NMR (100 MHz, $CDCl_3$) δ 199., 166.6, 160.7, 150.7, 140.6, 138.1, 133.6, 131.4, 131.2, 130.1, 125.8, 117.2, 51.0, 37.4, 35.7, 34.2, 27.6, 21.0, 13.7.

(2*Z*,4*E*,6*E*,8*E*)-methyl-9-(3-hydroxy-2,6,6-trimethylcyclohex-1-en-1-yl)-3,7-dimethylnona-2,4,6,8-tetraenoate (13)

In a 25 mL round bottom flask, **12** (2.50 g, 7.61 mmol) was dissolved in methanol (20 mL) and crystilline sodium borohydride (0.45 g, 11.9 mmol) was added slowly and left to stir at room temparature for 1 h where TLC analysis shows exhaustion of the starting material. Reaction mixture was diluted with water (25 mL), extraction done with CH_2Cl_2 (2 × 20 mL). Organic portions were mixed and concentrated to give a thick brownish oil. This was adsorbed on silica and packed on a column where elution was done via gravity using a solvent system of [petroleum ether/EtOAc (8:2)] to yield compound **13** as a yellow oil. Yield: 2.01 g (80%); ^{1}H

NMR (400 MHz, $CDCl_3$) δ 7.79 (d, *J* = 15.3 Hz, 1H), 7.03 – 6.92 (m, 1H), 6.27 (d, *J* = 11.4 Hz, 1H), 6.19 (d, *J* = 6.6 Hz, 2H), 5.66 (s, 1H), 4.01 (s, 1H), 3.71 (s, 3H), 2.07 (s, 3H), 1.99 (s, 3H), 1.90 (ddd, *J* = 11.5, 6.9, 3.1 Hz, 1H), 1.84 (s, 3H), 1.76 – 1.57 (m, 2H), 1.43 (ddd, *J* = 13.2, 7.3, 3.0 Hz, 1H), 1.05 (s, 3H), 1.02 (s, 3H). ^{13}C NMR (100 MHz, $CDCl_3$) δ 166.7, 151.1, 141.6, 139.2, 138.4, 132.0, 131.1, 130.2, 129.8, 127.5, 116.4, 70.2, 50.9, 34.8, 34.5, 29.0, 27.5, 20.9, 18.6, 12.8.

(2*Z*,4*E*,6*E*,8*E*)-methyl-9-(3-(1H-imidazol-1-yl)-2,6,6-trimethylcyclohex-1-en-1-yl)-3,7-dimethylnona-2,4,6,8-tetraenoate (14)

In a 25 mL round bottom flask **13,** (1.90 g, 5.75 mmol) was dissolved in acetonitrile (25 mL) followed by 1,1'-Carbonyldiimidazole (CDI) (1.21 mg, 7.47 mmol). On adding CDI, reaction mixture was seen to turn from yellow to dark red with evolution of gas. After 1 hr, TLC analysis showed exhaustion of starting material and the reaction mixture was therefore concentrated. Water (20 mL) was added and extraction was effected using with CH_2Cl_2 (3 × 20 mL). The combined organic portion was concentrated, adsorbed on silica and loaded on a column where elution was done via gravity with a solvent system of [methanol/CH_2Cl_2 (0.5:9.5)] to yield compound **14** as a red viscous oil. Yield: 1.50 g 69%; ^{1}H NMR (400 MHz, $CDCl_3$) δ 7.80 (d, *J* = 15.4 Hz, 1H), 7.50 (s, 1H), 7.07 (s, 1H), 7.00 – 6.87 (m, 2H), 6.33 – 6.17 (m, 3H), 5.67 (s, 1H), 4.54 (t, *J* = 4.8 Hz, 1H), 3.71 (s, 3H), 2.08 (s, 3H), 2.01 (s, 3H), 1.82 (dt, *J* = 35.3, 18.6 Hz, 2H), 1.61 (d, *J* = 10.8 Hz, 3H), 1.57 (d, *J* = 11.2 Hz, 1H), 1.50 (dd, *J* = 6.8, 3.5 Hz, 1H), 1.17 – 1.04 (m, 6H). ^{13}C NMR (100 MHz, $CDCl_3$) δ 166.7, 150.9, 144.8, 139.2, 138.6, 136.8, 131.7, 131.7, 130.2, 129.2, 126.5, 125.0, 118.1, 116.7, 77.3, 77.2, 77.0, 76.7, 58.0, 53.4, 51.0, 34.7, 34.6, 29.0, 28.1, 27.8, 20.9, 18.8, 12.8; HRMS (ESI) calcd for $C_{24}H_{32}N_2O_2Na^+$, 403.2355, Found: 403.2357.

General procedure A

(2*Z*,4*E*,6*E*,8*E*)-9-(3-(1H-imidazol-1-yl)-2,6,6-trimethylcyclohex-1-en-1-yl)-3,7-dimethylnona-2,4,6,8-tetraenoic acid (15)

In a 25 mL round bottom flask, **14** (1.00 g, 2.62 mmol) was dissolved in methanol/water (9:1) and pottassium hydroxide (final reaction concentration of 2M) was added. The reaction mixture was let to stir under reflux for 4 h after which the reaction mixture was concentrated and diluted with water (25 mL). The pH of the resulting solution was adjusted to 7. On adjusting the pH, compound **15** precipitated out of solution as a yellow solid, filtered and washed with cold ether (2 × 20 mL). This was used as is without further purification in the subsequent step. Yield: 0.60 g (63%); mp 151-153°C; ^{1}H NMR (400 MHz, $CDCl_3$) δ 12.07 (s, 1H), 7.78 – 7.61 (m, 2H), 7.17 – 6.87 (m, 3H), 6.32 (q, *J* = 16.2 Hz, 3H), 5.64 (s, 1H), 4.73 (s, 1H), 2.12 – 1.94 (m, 6H), 1.84 – 1.68 (m, 2H), 1.50 (s, 3H), 1.48 (s, 2H), 1.09 (d, *J* = 15.1 Hz, 6H). ^{13}C NMR (100 MHz, DMSO) δ 167.5, 150.6, 143.9, 139.5, 139.0, 137.3, 132.2, 131.9, 130.3, 128.6, 127.2, 125.8, 118.8, 118.2, 66.8, 35.1, 34.7, 29.1, 28.3, 28.1, 20.9, 18.8, 13.0; HRMS (ESI) calcd for $C_{23}H_{30}N_2O_2Na^+$, 389.2199, Found: 389.2202

General procedure B

(2*Z*,4*E*,6*E*,8*E*)-9-(3-(1H-imidazol-1-yl)-2,6,6-trimethylcyclohex-1-en-1-yl)-3,7-dimethyl-*N*-phenylnona-2,4,6,8-tetraenamide (16)

To a 25 mL round bottom flask, **15** (0.2 g, 0.546 mmol), aniline (0.056 g, 0.601 mmol), EDC (0.208 g, 1.09 mmol), HOBT (0.147 g, 1.09mmol) and DIPEA (0.706 g, 5.46 mmol) were dissolved in DMF (3 mL).The reaction mixture was allowed to stir for 12 h, concentrated, diluted with water (50 mL) and extracted using CH_2Cl_2 (3 × 20 mL). The combined organic portions

were dried over Na_2SO_4, and concentrated to give the crude product as a reddish oil. Purification by gravity chromatography on silica using 10 % EtOAc in petroleum ether gave **16** as a yellow powder. Yield: 0.16 g (64%); mp: 166-168°C; ^{1}H NMR (400 MHz, $CDCl_3$) δ 7.93 (d, *J* = 15.5 Hz, 1H), 7.52 (d, *J* = 16.1 Hz, 3H), 7.33 (t, *J* = 7.7 Hz, 2H), 7.26 (s, 3H), 7.21 (s, 1H), 7.14 – 7.06 (m, 2H), 6.94 (dd, *J* = 15.3, 11.3 Hz, 2H), 6.31 (d, *J* = 11.5 Hz, 1H), 6.21 (q, *J* = 16.0 Hz, 2H), 5.70 (s, 1H), 4.54 (s, 1H), 2.09 (s, 3H), 2.01 (s, 3H), 1.92 (s, 1H), 1.85 (s, 1H), 1.66 (s, 3H), 1.57 (d, *J* = 18.1 Hz, 4H), 1.50 (s, 1H), 1.37 – 1.26 (m, 1H), 1.17 – 1.02 (m, 6H). ^{13}C NMR (100 MHz, $CDCl_3$) δ 164.6, 154.1, 146.9, 145.2, 139.5, 137.4, 136.5, 132.3, 131.1, 130.4, 130.2, 128.4, 125.7, 124.5, 121.7, 120.9, 118.5, 115.7, 53.4, 36.5, 31.4, 29.0, 27.7, 24.9, 20.8, 18.8, 12.7; HRMS (ESI) calcd for $C_{29}H_{35}N_3ONa^+$, 464.2672. Found: 464.2674.

(2*Z*,4*E*,6*E*,8*E*)-9-(3-(1H-imidazol-1-yl)-2,6,6-trimethylcyclohex-1-en-1-yl)-*N*-(4-hydroxyphenyl)-3,7-dimethylnona-2,4,6,8-tetraenamide (17)

Compound **17** was synthesized using general procedure B. Yellow powder. Yield: 0.113 g (47%); mp: 111-113°C; ^{1}H NMR (400 MHz, $CDCl_3$) δ 8.22 (s, 1H), 7.53 (s, 1H), 7.42 (d, *J* = 7.9 Hz, 1H), 7.08 (s, 1H), 6.93 (s, 1H), 6.85 (dd, *J* = 21.5, 10.1 Hz, 3H), 6.27 – 6.08 (m, 2H), 5.76 (s, 1H), 4.54 (s, 1H), 3.47 (s, 1H), 2.09 (d, *J* = 11.4 Hz, 1H), 2.02 (s, 2H), 1.98 (s, 3H), 1.91 (s, *J* = 22.5 Hz, 5H), 1.85 (d, *J* = 17.8 Hz, 1H), 1.65 (d, *J* = 12.6 Hz, 1H), 1.56 (d, *J* = 15.3 Hz, 3H), 1.50 (d, *J* = 5.6 Hz, 1H), 1.31 (dd, *J* = 26.4, 14.7 Hz, 1H), 1.11 (s, 3H), 1.07 (s, 3H). ^{13}C NMR (100 MHz, $CDCl_3$) δ 164.6, 154.1, 146.9, 145.2, 139.5, 137.4, 136.5, 132.3, 131.1, 130.4, 130.2, 128.4, 125.7, 124.5, 121.7, 120.9, 118.5, 115.7, 53.4, 36.5, 31.4, 29.0, 27.7, 24.9, 20.8, 18.8, 12.7; HRMS (ESI) calcd for $C_{29}H_{35}N_3O_2Na^+$, 480.2621. Found: 480.2624.

(2*Z*,4*E*,6*E*,8*E*)-9-(3-(1H-imidazol-1-yl)-2,6,6-trimethylcyclohex-1-en-1-yl)-*N*-(2-hydroxyphenyl)-3,7-dimethylnona-2,4,6,8-tetraenamide (18)

Compound **18** was synthesized using general procedure B. Yellow powder. Yield: 0.080 g (32%); mp: 136-138°C; ^{1}H NMR (400 MHz, $CDCl_3$) δ 7.93 (d, *J* = 15.6 Hz, 1H), 7.66 (s, 1H), 7.50 (s, 1H), 7.16 – 6.79 (m, 7H), 6.32 (d, *J* = 11.4 Hz, 1H), 6.23 (d, *J* = 7.3 Hz, 2H), 5.78 (s, 1H), 4.54 (s, 1H), 2.09 (d, *J* = 16.3 Hz, 3H), 2.02 (s, 3H), 1.85 (s, 2H), 1.59 (s, 4H), 1.52 (d, *J* = 15.8 Hz, 2H), 1.11 (d, *J* = 21.1 Hz, 6H).^{13}C NMR (100 MHz, $CDCl_3$) δ 165.9, 149.9, 149.0, 144.9, 139.2, 138.8, 136.7, 131.9, 130.2, 129.0, 126.7, 126.5, 126.1, 125.0, 121.8, 120.1, 119.4, 118.3, 58.0, 34.7, 34.6, 29.0, 28.1, 27.8, 21.1, 18.8, 12.9; HRMS (ESI) calcd for $C_{29}H_{35}N_3O_2Na^+$, 480.2621. Found: m/z = 480.2626.

(2*Z*,4*E*,6*E*,8*E*)-9-(3-(1H-imidazol-1-yl)-2,6,6-trimethylcyclohex-1-en-1-yl)-*N*-(4-fluorophenyl)-3,7-dimethylnona-2,4,6,8-tetraenamide (19)

Compound **19** was synthesized using general procedure B. Yellow powder. Yield: 0.151 g (63%); mp: 123-125°C; 1H NMR (400 MHz, CDCl3) δ 8.22 (s, 1H), 7.53 (s, 1H), 7.42 (d, *J* = 7.9 Hz, 1H), 7.08 (s, 1H), 6.93 (s, 1H), 6.75 (dd, *J* = 21.5, 10.1 Hz, 3H), 6.41 (m, 2H), 5.76 (s, 1H), 4.54 (s, 1H), 3.47 (s, 1H), 2.09 (d, *J* = 11.4 Hz, 1H), 2.02 (s, 2H), 1.98 (s, 3H), 1.91 (s, *J* = 22.5 Hz, 5H), 1.85 (d, *J* = 17.8 Hz, 1H), 1.65 (d, *J* = 12.6 Hz, 1H), 1.56 (d, *J* = 15.3 Hz, 3H), 1.50 (d, *J* = 5.6 Hz, 1H), 1.31 (dd, *J* = 26.4, 14.7 Hz, 1H), 1.11 (s, 3H), 1.07 (s, 3H). 13C NMR (100 MHz, CDCl3) δ 164.7, 153.1, 146.8, 145.2, 139.5, 137.4, 135.5, 132.3, 131.0, 130.4, 130.2, 127.4, 125.7, 124.5, 122.7, 120.9, 116.5, 115.7, 53.4, 35.5, 31.4, 29.0, 27.7, 24.9, 20.8, 18.8, 12.7; calcd for $C_{29}H_{34}FN_3ONa^+$, 482.2578. Found: m/z = 482.2580.

(2*Z*,4*E*,6*E*,8*E*)-9-(3-(1H-imidazol-1-yl)-2,6,6-trimethylcyclohex-1-en-1-yl)-*N*-(3-fluorophenyl)-3,7-dimethylnona-2,4,6,8-tetraenamide (20)

Compound **20** was synthesized using general procedure B. Yellow powder. Yield: 0.143 g (59%); mp: 119-121°C; ^{1}H NMR (400 MHz, $CDCl_3$) δ 7.92 (d, *J* = 15.4 Hz, 1H), 7.51 (dd, *J* = 33.6, 17.3 Hz, 3H), 7.17 (s, 1H), 7.07 (s, 1H), 7.03 – 6.88 (m, 2H), 6.78 (s, 1H), 6.34 – 6.14 (m, 3H), 5.68 (s, 1H), 4.54 (s, 1H), 2.05 (d, *J* = 32.2 Hz, 6H), 1.85 (s, 1H), 1.69 (s, 3H), 1.52 (d, *J* = 17.0 Hz, 2H), 1.29 (s, 1H), 1.10 (d, *J* = 19.9 Hz, 6H) ^{13}C NMR (100 MHz, $CDCl_3$) δ 164.4, 161.8, 149.0, 144.9, 139.9, 139.2, 138.4, 136.8, 136.2, 131.9, 131.4, 131.0, 130.4, 130.0, 129.9, 129.1, 126.4, 125.0, 119.5, 118.2, 58.0, 34.7, 34.6, 29.03, 28.1, 27.8, 21.0, 18.8, 12.8; HRMS (ESI) calcd for $C_{29}H_{34}FN_3ONa^+$, 482.2578. Found: 482.2580.

(2*Z*,4*E*,6*E*,8*E*)-9-(3-(1H-imidazol-1-yl)-2,6,6-trimethylcyclohex-1-en-1-yl)-*N*-benzyl-3,7-dimethylnona-2,4,6,8-tetraenamide (21)

Compound **21** was synthesized using general procedure B. Yellow powder. Yield: 0.124 g (52%); mp: 79-81°C; ^{1}H NMR (400 MHz, $CDCl_3$) δ 7.89 (d, *J* = 3.3 Hz, 1H), 7.71 – 7.65 (m, 2H), 7.37 (dd, *J* = 14.1, 6.2 Hz, 1H), 7.34 – 7.28 (m, 5H), 7.09 (s, 1H), 6.92 (s, 1H), 6.28 (d, *J* = 11.2 Hz, 1H), 6.18 (d, *J* = 5.8 Hz, 1H), 5.79 (s, 1H), 5.58 (s, 1H), 4.58 (s, 1H), 4.49 (d, *J* = 5.7 Hz, 2H), 2.16 – 2.08 (m, 1H), 2.06 – 1.97 (m, 6H), 1.82 (dd, *J* = 8.8, 4.2 Hz, 1H), 1.61 – 1.53 (m, 3H), 1.52 – 1.47 (m, 2H), 1.15 (d, 6H). ^{13}C NMR (100 MHz, $CDCl_3$) δ 166.2, 146.8, 146.0, 139.5, 138.4, 137.5, 136.1, 132.3, 130., 130.38, 128.7, 127.8, 127.4, 126.0, 125.6, 124.1, 123.8, 120., 119.0, 110.1, 58.7, 43.5, 34.7, 34.3, 29.0, 28.0, 27.7, 20.8, 18.8, 12; calcd for $C_{30}H_{37}N_3ONa^+$, 478.2828. Found: 478.2829.

(2*Z*,4*E*,6*E*,8*E*)-9-(3-(1H-imidazol-1-yl)-2,6,6-trimethylcyclohex-1-en-1-yl)-*N*-(4-hydroxybenzyl)-3,7-dimethylnona-2,4,6,8-tetraenamide (22)

Compound **22** was synthesized using general procedure B. Yellow powder. Yield: 0.161 g (62%); mp: 139-141°C; ^{1}H NMR (400 MHz, $CDCl_3$) δ 7.66 (d, *J* = 15.3 Hz, 1H), 7.55 (s, 1H), 7.14 (d, *J* = 7.5 Hz, 2H), 7.09 (s, 1H), 6.95 (s, 1H), 6.87 – 6.77 (m, 3H), 6.17 (dd, *J* = 18.0, 10.5 Hz, 3H), 5.94 (s, 1H), 5.62 (s, 1H), 4.54 (s, 1H), 4.48 – 4.29 (m, 2H), 2.14 (s, 1H), 1.97 (t, *J* = 6Hz, 6H), 1.85 (s, 2H), 1.60 (s, 3H), 1.53 (d, *J* = 12.8 Hz, 2H), 1.10 (s, 6H). ^{13}C NMR (100 MHz, $CDCl_3$) δ 166.4, 156.9, 145.6, 145.2, 140.0, 137.2, 136.2, 132.5, 131.0, 129.8, 129.3, 128.9, 128.2, 125.5, 124.4, 121.1, 118.8, 115.8, 58.5, 43.2, 34.6, 34.4, 29.0, 28.0, 27.8, 20.5, 19.1, 12.7; HRMS (ESI) calcd for $C_{30}H_{37}N_3O_2Na^+$, 494.2777. Found: 494.2780.

(2Z,4E,6E,8E)-9-(3-(1H-imidazol-1-yl)-2,6,6-trimethylcyclohex-1-en-1-yl)-N-(4-fluorobenzyl)-3,7-dimethylnona-2,4,6,8-tetraenamide (23).

Compound **23** was synthesized using general procedure B .Yellow powder. Yield: 0.119 g (47%); mp: 93-95 °C; ^{1}H NMR (400 MHz, $CDCl_3$) δ 7.95 – 7.84 (m, 2H), 7.74 – 7.65 (m, 1H), 7.12 (s, 1H), 6.93 (ddd, *J* = 26.9, 16.4, 10.0 Hz, 4H), 6.22 (dt, *J* = 22.8, 13.7 Hz, 4H), 5.86 (s, 1H), 5.59 (s, 1H), 4.58 (d, *J* = 4.6 Hz, 1H), 4.45 (d, *J* = 5.8 Hz, 2H), 2.18 – 2.07 (m, 1H), 2.05 – 1.96 (m, 6H), 1.83 (dd, *J* = 9.1, 4.8 Hz, 1H), 1.58 (s, 3H), 1.53 – 1.49 (m, 2H), 1.15 – 1.06 (m, 6H). ^{13}C NMR (100 MHz, $CDCl_3$) δ 166.2, 164.8, 163.4, 150.6, 147.0, 146.7, 139.5, 137.6, 134.3, 132.2, 130.9, 130.4, 129.5, 129.4, 125.6, 123.9, 123.9, 122.0,115.6, 115.4, 110.1, 58.8, 42.7, 34.7, 34.2, 29.0, 28.0, 27.7, 20.8, 18.8, 12.8; calcd for $C_{30}H_{36}FN_3ONa^+$, 496.2734. Found: 496.2735.

(2Z,4E,6E,8E)-9-(3-(1H-imidazol-1-yl)-2,6,6-trimethylcyclohex-1-en-1-yl)-*N*-(3-fluorobenzyl)-3,7-dimethylnona-2,4,6,8-tetraenamide (24)

Compound **24** was synthesized using general procedure B. Yellow powder. Yield: 0.137 g (54%); mp: 96-98°C; ^{1}H NMR (400 MHz, $CDCl_3$) δ 7.93 – 7.86 (m, 1H), 7.69 (s, 1H), 7.15 – 6.84 (m, 7H), 6.28 (d, *J* = 11.4 Hz, 1H), 6.26 – 6.12 (m, 2H), 5.91 (s, 1H), 5.60 (s, 1H), 4.58 (d, *J* = 4.5 Hz, 1H), 4.49 (d, *J* = 5.9 Hz, 2H), 2.19 – 2.07 (m, 1H), 2.02 (d, *J* = 18.1 Hz, 6H), 1.83 (dd, *J* = 9.5, 5.5 Hz, 1H), 1.58 (s, 3H), 1.50 (dd, *J* = 15.4, 9.4 Hz, 2H), 1.16 – 1.05 (m, 6H). ^{13}C NMR (100 MHz, $CDCl_3$) δ 166.2, 164.2, 161.7, 147.2, 145.9, 141.2, 139.5, 137.7, 132.2, 130.9, 130.5, 130.1, 125.7, 124.0, 123.2, 119.7, 114.6, 110.0, 58.6, 42.8, 34.7, 34.3, 29.0, 27.9, 27.7, 20.8, 18.8, 12.8; calcd. for $C_{30}H_{36}FN_3ONa^+$, 496.2734. Found: 496.2735.

(2*Z*,4*E*,6*E*,8*E*)-9-(3-(1H-imidazol-1-yl)-2,6,6-trimethylcyclohex-1-en-1-yl)-*N*-(4-hydroxyphenethyl)-3,7-dimethylnona-2,4,6,8-tetraenamide (25)

Compound **25** was synthesized using general procedure B. Yellow powder. Yield: 0.161 g (60%); mp: 126-128°C; ^{1}H NMR (400 MHz, $CDCl_3$) δ 7.58 (d, *J* = 15.3 Hz, 1H), 7.10 (s, 1H), 7.04 (d, *J* = 8.4 Hz, 2H), 6.94 (s, 1H), 6.85 – 6.80 (m, 3H), 6.23 – 6.16 (m, 4H), 5.60 (t, *J* = 5.7 Hz, 1H), 5.54 (s, 1H), 4.55 (t, *J* = 4.7 Hz, 1H), 3.57 – 3.51 (m, 2H), 2.76 (t, *J* = 6.7 Hz, 2H), 2.17 – 2.07 (m, 1H), 1.98 (dd, *J* = 9.1, 5.3 Hz, 6H), 1.88 – 1.77 (m, 2H), 1.60 (s, 3H), 1.51 (dd, *J* = 14.0, 3.9 Hz, 2H), 1.10 (d, *J* = 9.6 Hz, 6H). ^{13}C NMR (100 MHz, $CDCl_3$) δ 166.7, 155.3, 145.9, 145.4, 139.7, 137.4, 132.2, 130.7, 130.1, 129.7, 125.9, 125.6, 124.0, 124.0, 121.0, 119.0, 115.7, 110.2, 58.6, 40.7, 34.7, 34.3, 29.1, 28.0, 27.6, 20.7, 19.0, 12.7; calcd for $C_{31}H_{39}N_3O_2Na^+$, 508.2934. Found: 508.2935.

(2*Z*,4*E*,6*E*,8*E*)-methyl 3,7-dimethyl-9-(2,6,6-trimethyl-3-(trifluoromethyl)sulfonyl)oxy) cyclohexa-1,3-dien-1-yl)nona-2,4,6,8-tetraenoate (26)

In a 50 mL flask equipped with a magnetic stirrer, THF (10 mL) was added and the temperature lowered to -78°C. Sodium bis(trimethylsilyl)amide solution ((1M in THF), 9.2 mL,9.24 mmol) was added into the chilled THF. On to this, **12** (2.0 g, 6.09 mmol) dissolved in 10 mL THF was added very slowly and let to stir for 45 min at this temparature. During this time, reaction mixture was seen to turn from yellow color to brick red. N-(5-chloro-2-pyridyl)bis trifluoromethanesulfonimide (3.58 g, 9.12 mmol) dissolved in 10 mL THF was added very slowly onto the reaction mixture. Reaction mixure was then let to stir at this temperature for an additional 3 h. Reaction mixture was thereafter poured quickly into an aqueous solution of $NaHCO_3$ and extracted using EtOAc. Purification by flash chromatography on silica using 10 % EtOAc in petroleum ether gave **26** as a yellow powder. Yield: 2.03 g (75%); mp: 98-100 °C; ^{1}H NMR (400 MHz, $CDCl_3$) δ 7.82 (d, *J* = 15.3 Hz, 1H), 6.97 (dd, *J* = 15.3, 11.4 Hz, 1H), 6.37 – 6.11 (m, 3H), 5.73 (t, *J* = 4.9 Hz, 1H), 5.68 (s, 1H), 3.71 (d, *J* = 2.7 Hz, 3H), 2.24 (d, *J* = 5.0 Hz, 2H), 2.08 (d, *J* = 1.1 Hz, 3H), 2.01 (s, 3H), 1.90 (s, 3H), 1.06 (s, 6H). ^{13}C NMR (100 MHz, $CDCl_3$) δ 166.7, 150.8, 147.9, 144.5, 139.1, 138.5, 132.5, 131.6, 130.6, 125.4, 122.0, 120.1, 116.9, 113.8, 51.0, 37.7, 34.5, 26.3, 20.9, 14.4, 12.7; calcd for $C_{22}H_{27}F_3O_5SNa^+$, 483.1423. Found: 483.1422.

General procedure C.

(2*Z*,4*E*,6*E*,8*E*)-methyl-9-(3'-methoxy-2,4,4-trimethyl-4,5-dihydro-[1,1'-biphenyl]-3-yl)-3,7-dimethylnona-2,4,6,8-tetraenoate (27)

In a 50 ml flask, $CeCO_3$ (2.11 g, 6.47 mmol) dissolve in I mL was added followed by 10 mL of dioxane. The solution was flushed with N_2 for 1 h. **19** (1.92 g, 4.31 mmol), 3-methoxyphenylboronic acid (0.787 g, 5.18mmol) and lastly $Pd(Ph_3)_4$ (5% weight of 18) were added onto the flask and the reaction mixture allowed to reflux at 85°C for 12 h. The reaction mixture was concentrated and brine was added. Extraction was done using EtOAc and the organic extracts were concentrated to give a crude product as a dark yellow oil. Purification by gravity chromatography on silica using 5 % EtOAc in petroleum ether gave **27** as a red oil. Yield: 1.60 g (88%); ^{1}H NMR (400 MHz, $CDCl_3$) δ 7.80 (d, *J* = 15.3 Hz, 1H), 7.27 – 7.21 (m, 1H), 6.99 (dd, *J* = 15.3, 11.5 Hz, 1H), 6.84 – 6.76 (m, 2H), 6.73 (dd, *J* = 2.3, 1.6 Hz, 1H), 6.35 (s, 2H), 6.32 (d, *J* = 11.6 Hz, 1H), 5.76 (t, *J* = 4.7 Hz, 1H), 5.65 (s, 2H), 3.86 (s, 1H), 3.81 (d, *J* = 1.8 Hz, 3H), 3.70 (s, 3H), 2.18 (d, *J* = 4.8 Hz, 2H), 2.07 (d, *J* = 1.0 Hz, 3H), 2.03 (s, 3H), 1.74 (s, 3H), 1.10 (d, *J* = 5.8 Hz, 6H). ^{13}C NMR (100 MHz, $CDCl_3$) δ 166.7, 159.2, 151.1, 143.6, 141.6, 140.9, 139.5, 137.4, 132.1, 131.2, 129.7, 128.8, 127.7, 127.4, 124.6, 120.9, 116.3, 114.0, 111.9, 55.2, 50.9, 39.6, 34.3, 26.6, 20.9, 18.8, 12.8; calcd for $C_{28}H_{34}O_3Na^+$, 441.2400. Found: 441.24.

(2*Z*,4*E*,6*E*,8*E*)-methyl-3,7-dimethyl-9-(2,6,6-trimethyl-3-(pyridin-3-yl)cyclohexa-1,3-dien-1-yl)nona-2,4,6,8-tetraenoate (28)

Compound **28** was synthesized using general procedure C using the respective boronic acid. Yellow powder. Yield: 1.201 g (69%); mp: 77-79 °C; ^{1}H NMR (400 MHz, $CDCl_3$) δ 8.54 – 8.44 (m, 2H), 7.80 (d, *J* = 15.3 Hz, 1H), 7.57 – 7.45 (m, 1H), 7.27 – 7.22 (m, 1H), 6.99 (dd, *J* = 15.3, 11.4 Hz, 1H), 6.32 (d, *J* = 10.5 Hz, 3H), 5.79 (t, *J* = 4.8 Hz, 1H), 5.66 (s, 1H), 3.71 (d, *J* = 3.0 Hz, 3H), 2.22 (t, *J* = 5.8 Hz, 2H), 2.08 (d, *J* = 1.0 Hz, 3H), 2.03 (s, 3H), 1.71 (s, 3H), 1.11 (d, *J* = 6.1 Hz, 6H). ^{13}C NMR (100 MHz, $CDCl_3$) δ 166.7, 151.1, 149.2, 147.8, 141.6, 139.3, 138.4,

137.8, 137.6, 135.6, 132.0, 131.4, 129.9, 126.9, 126.5, 126.3, 122.7, 116.4, 50.9, 39.5, 34.3, 26.7, 26.6, 20.9, 18.8, 12.8; calcd for $C_{26}H_{31}NO_2Na^+$, 412.2247. Found: 412.2247.

(2*Z*,4*E*,6*E*,8*E*)-methyl-3,7-dimethyl-9-(2,6,6-trimethyl-3-(pyrimidin-5-yl)cyclohexa-1,3-dien-1-yl)nona-2,4,6,8-tetraenoate (29)

Compound **29** was synthesized using general procedure C using the respective boronic acid. Yellow powder. Yield: 0.896 g (60%) ; mp: 162-164 °C; ^{1}H NMR (400 MHz, $CDCl_3$) δ 9.13 (s, 1H), 8.61 (d, *J* = 3.9 Hz, 2H), 7.81 (d, *J* = 15.3 Hz, 1H), 6.99 (dd, *J* = 15.3, 11.4 Hz, 1H), 6.33 (t, *J* = 5.6 Hz, 3H), 5.85 (t, *J* = 4.7 Hz, 1H), 5.67 (s, 1H), 3.71 (s, 3H), 2.25 (d, *J* = 4.8 Hz, 2H), 2.08 (d, *J* = 0.8 Hz, 3H), 2.04 (d, *J* = 5.0 Hz, 3H), 1.73 (s, 3H), 1.11 (d, *J* = 5.7 Hz, 6H). ^{13}C NMR (100 MHz, $CDCl_3$) δ 166.7, 157.0, 155.8, 151.0, 142.4, 139.0, 138.2, 135.4, 135.2, 131.8, 131.7, 130.1, 128.0, 126.5, 125.2, 116.6, 50.9, 39.4, 34.3, 26.6, 26.6, 20.9, 18.8, 12.8; calcd for $C_{25}H_{30}N_2O_2Na^+$, 413.2199. Found: 413.2199.

(2*Z*,4*E*,6*E*,8*E*)-9-(3'-methoxy-2,4,4-trimethyl-4,5-dihydro-[1,1'-biphenyl]-3-yl)-3,7-dimethylnona-2,4,6,8-tetraenoic acid (30)

Compound **30** was synthesized using the general procedure A .Yellow powder. Yield: 0.621 g (62%); mp: 194-196°C; ^{1}H NMR (400 MHz, $CDCl_3$) δ 7.76 (t, *J* = 14.0 Hz, 1H), 7.22 (t, *J* = 7.9 Hz, 1H), 7.03 (dd, *J* = 15.3, 11.5 Hz, 1H), 6.82 – 6.75 (m, 2H), 6.73 (d, *J* = 1.7 Hz, 1H), 6.39 – 6.31 (m, 3H), 5.76 (t, *J* = 4.7 Hz, 1H), 5.68 (s, 1H), 3.81 (d, *J* = 3.0 Hz, 3H), 2.18 (t, *J* = 6.4 Hz, 2H), 2.11 (s, 3H), 2.03 (s, 3H), 1.73 (s, 3H), 1.11 (d, *J* = 7.1 Hz, 6H). ^{13}C NMR (100 MHz, $CDCl_3$) δ 166.7, 159.2, 151.1, 143.6, 141.6, 140.9, 139.5, 137.4, 132.1, 131.2, 129.7, 128.8,

127.6, 127.4, 124.6, 120.9, 116.3, 113.9, 111.9, 55.2, 50.9, 39.6, 34.3, 26.7, 26.6, 20.9, 18.8, 12.8; calcd for $C_{27}H_{32}O_3Na^+$, 427.2243. Found: m/z = 427.2246.

(2*Z*,4*E*,6*E*,8*E*)-3,7-dimethyl-9-(2,6,6-trimethyl-3-(pyridin-3-yl)cyclohexa-1,3-dien-1-yl)nona-2,4,6,8-tetraenoic acid (31)

Compound **31** was synthesized using general procedure A. Orange powder. Yield: 0.584 g (48%); mp: 113-116 °C; ^{1}H NMR (400 MHz, $CDCl_3$) δ 8.54 – 8.44 (m, 2H), 7.81 (d, *J* = 15.3 Hz, 1H), 7.53 (dt, *J* = 7.8, 1.9 Hz, 1H), 7.31 – 7.22 (m, 1H), 7.01 (dd, *J* = 15.3, 11.5 Hz, 1H), 6.34 (d, *J* = 9.6 Hz, 3H), 5.78 (t, *J* = 4.7 Hz, 1H), 5.71 (s, 1H), 2.21 (d, *J* = 4.8 Hz, 2H), 2.10 (t, *J* = 3.4 Hz, 3H), 2.04 (d, *J* = 5.0 Hz, 3H), 1.70 (s, 3H), 1.11 (d, *J* = 8.8 Hz, 6H). ^{13}C NMR (100 MHz, $CDCl_3$) δ 169.3, 152.5, 148.6, 147.2, 141.7, 139.5, 138.2, 137.8, 136.1, 132.3, 131.5, 129.9, 127.1, 126.6, 126.4, 122.9, 116.3, 77.3, 77.2, 77.0, 76.7, 39.5, 34.3, 26.6, 21.1, 18.8, 12.8; calcd for $C_{25}H_{29}NO_2Na^+$, 398.2090. Found: 398.2090.

(2*Z*,4*E*,6*E*,8*E*)-3,7-dimethyl-9-(2,6,6-trimethyl-3-(pyrimidin-5-yl)cyclohexa-1,3-dien-1-yl)nona-2,4,6,8-tetraenoic acid (32)

Compound **32** was synthesized using general procedure A. Yellow powder. Yield: 0.673 g (70%); mp: 111-113 °C; ^{1}H NMR (400 MHz, $CDCl_3$) δ 9.13 (d, *J* = 3.6 Hz, 1H), 8.62 (d, *J* = 5.5 Hz, 2H), 7.80 (d, *J* = 15.3 Hz, 1H), 7.02 (dd, *J* = 15.3, 11.5 Hz, 1H), 6.41 – 6.29 (m, 3H), 5.85 (t, *J* = 4.7 Hz, 1H), 5.70 (s, 1H), 2.25 (d, *J* = 4.8 Hz, 2H), 2.11 (t, *J* = 3.6 Hz, 3H), 2.04 (d, *J* = 3.8 Hz, 3H), 1.73 (s, 3H), 1.11 (d, *J* = 7.4 Hz, 6H). ^{13}C NMR (100 MHz, $CDCl_3$) δ 169.7, 156.8, 155.8, 153.0, 142.4, 139.5, 138.2, 135.5, 135.1, 132.4, 131.7, 130.0, 128.2, 126.7, 125.3, 116.0, 67.1, 39.4, 34.3, 26.6, 21.1, 18.8, 12.8; calcd for $C_{24}H_{28}N_2O_2Na^+$, 399.2042. Found: 399.2043.

(2*Z*,4*E*,6*E*,8*E*)-*N*-(4-hydroxybenzyl)-9-(3'-methoxy-2,4,4-trimethyl-4,5-dihydro-[1,1'-biphenyl]-3-yl)-3,7-dimethylnona-2,4,6,8-tetraenamide (33)

Compound **33** was synthesized using general procedure B as a red oil. Yield: 0.124 g (45%); ^{1}H NMR (400 MHz, $CDCl_3$) δ 7.21 – 7.14 (m, 2H), 6.83 – 6.69 (m, 5H), 6.35 – 6.13 (m, 4H), 5.77 – 5.52 (m, 4H), 4.92 (d, *J* = 5.7 Hz, 1H), 4.42 (d, *J* = 5.6 Hz, 2H), 3.83 (t, *J* = 7.8 Hz, 3H), 2.18 (t, *J* = 5.3 Hz, 3H), 2.02 (d, *J* = 6.8 Hz, 3H), 1.75 (d, *J* = 11.6 Hz, 3H), 1.10 (dd, *J* = 11.3, 5.9 Hz, 6H). ^{13}C NMR (100 MHz, $CDCl_3$) δ 166.5, 159.2, 155.5, 149.1, 147.0, 143.7, 141.6, 141.0, 138.6, 137.6, 135.8, 132.3, 131.4, 130.8, 130.1, 129.3, 128.8, 127.5, 126.9, 124.5, 120.9, 119.5, 115.6, 113.9, 111.9, 55.2, 43.0, 39.5, 36.6, 34.3, 26.6, 20.8, 18.8, 12.8; calcd for $C_{34}H_{39}NO_3Na^+$, 532.2822. Found: 532.2821.

(2*Z*,4*E*,6*E*,8*E*)-*N*-(4-hydroxyphenethyl)-9-(3'-methoxy-2,4,4-trimethyl-4,5-dihydro-[1,1'-biphenyl]-3-yl)-3,7-dimethylnona-2,4,6,8-tetraenamide (34)

Compound **34** was synthesized using general procedure B. Yellow powder. Yield: 0.104 g (40%); mp: 102-105 °C; ^{1}H NMR (400 MHz, $CDCl_3$) δ 7.76 (d, *J* = 15.3 Hz, 1H), 7.23 (t, *J* = 7.9 Hz, 1H), 7.06 (d, *J* = 8.4 Hz, 2H), 6.88 (dd, *J* = 15.3, 11.4 Hz, 1H), 6.80 (dd, *J* = 14.0, 5.4 Hz, 4H), 6.73 (s, 1H), 6.32 (s, 2H), 6.27 (d, *J* = 11.5 Hz, 1H), 5.75 (t, *J* = 4.6 Hz, 1H), 5.46 (d, *J* = 11.5 Hz, 2H), 5.09 (s, 1H), 3.82 (s, 3H), 3.53 (dd, *J* = 12.9, 6.7 Hz, 2H), 2.77 (t, *J* = 6.9 Hz, 2H), 2.18 (t, *J* = 5.1 Hz, 2H), 1.99 (d, *J* = 8.2 Hz, 6H), 1.73 (s, 3H), 1.56 (s, 3H), 1.10 (d, *J* = 4.8 Hz, 6H). ^{13}C NMR (100 MHz, $CDCl_3$) δ 200.9, 191.8, 166.6, 159.2, 154.4, 146.5, 143.7, 141.6, 141.0, 138.5, 137.6, 131.4, 130.8, 130.7, 130.1, 129.8, 128.8, 127.4, 126.8, 125.2, 124.5, 120.9, 119.9, 115.5, 113.9, 111.9, 109.3, 55.2, 40.7, 39.5, 34.8, 34.3, 26.6, 20.8, 18.8, 12.7; calcd for $C_{35}H_{41}NO_3Na^+$, 546.2978. Found: 546.2977.

(2*Z*,4*E*,6*E*,8*E*)-3,7-dimethyl-*N*-phenyl-9-(2,6,6-trimethyl-3-(pyridin-3-yl)cyclohexa-1,3-dien-1-yl)nona-2,4,6,8-tetraenamide (35)

Compound **35** was synthesized using general procedure B. Yellow powder. Yield: 0.149 g (62%); mp: 102-104 °C; ^{1}H NMR (400 MHz, $CDCl_3$) δ 8.51 (dd, *J* = 4.8, 1.6 Hz, 1H), 8.47 (d, *J* = 1.6 Hz, 1H), 7.92 (d, *J* = 15.5 Hz, 1H), 7.55 (d, *J* = 7.1 Hz, 2H), 7.53 – 7.48 (m, 1H), 7.32 (t, *J* = 7.9 Hz, 3H), 7.17 (s, 1H), 7.11 (d, *J* = 7.4 Hz, 1H), 6.96 (dd, *J* = 15.1, 11.4 Hz, 1H), 6.35 (s, 1H), 6.32 (s, 2H), 5.79 (t, *J* = 4.7 Hz, 1H), 5.68 (s, 1H), 2.21 (d, *J* = 4.8 Hz, 2H), 2.09 (s, 3H), 2.02 (s, 3H), 1.71 (d, *J* = 4.6 Hz, 3H), 1.11 (d, *J* = 7.4 Hz, 6H) ^{13}C NMR (100 MHz, $CDCl_3$) δ 166.8, 158.2, 149.2, 148.4, 147.8, 141.6, 138.8, 138.4, 137.9, 137.6, 135.6, 131.6, 131.3, 130.2, 128.9, 126.7, 126.3, 122.7, 39.5, 34.3, 26.6, 20.9, 18.8, 12.8; calcd for $C_{31}H_{34}N_2ONa^+$, 473.2563. Found: 473.2563.

(2*Z*,4*E*,6*E*,8*E*)-*N*-(4-hydroxybenzyl)-3,7-dimethyl-9-(2,6,6-trimethyl-3-(pyridin-3-yl)cyclohexa-1,3-dien-1-yl)nona-2,4,6,8-tetraenamide (36)

Compound **36** was synthesized using general procedure B. Yellow powder. Yield: 0.104 g (80%); mp: 124-126 °C; ^{1}H NMR (400 MHz, $CDCl_3$) δ 8.52 – 8.42 (m, 2H), 7.78 (d, *J* = 15.0 Hz, 1H), 7.62 – 7.49 (m, 2H), 7.16 (d, *J* = 8.5 Hz, 2H), 6.82 (q, *J* = 3.0 Hz, 2H), 6.31 – 6.22 (m, 3H), 5.79 (dd, *J* = 12.5, 7.8 Hz, 2H), 5.57 (s, 1H), 4.41 (d, *J* = 5.7 Hz, 2H), 2.21 (d, *J* = 4.8 Hz, 2H), 2.01 (d, *J* = 5.1 Hz, 6H), 1.71 (s, 3H), 1.10 (d, *J* = 7.3 Hz, 6H). ^{13}C NMR (100 MHz, DMSO) δ 165.8, 156.7, 148.9, 148.2, 145.3, 141.8, 138.5, 138.3, 138.2, 137.4, 135.9, 132.2, 131.5, 130.2, 129.1, 126.4, 126.3, 126.3, 123.6, 123.5, 121.5, 118.8, 115.4, 111.0, 41.9, 34.3, 26.8, 20.9, 19.0, 12.9; calcd for $C_{32}H_{36}N_2O_2Na^+$, 503.2669. Found: 503.2667.

(2*Z*,4*E*,6*E*,8*E*)-*N*-(4-hydroxyphenethyl)-3,7-dimethyl-9-(2,6,6-trimethyl-3-(pyridin-3-yl)cyclohexa-1,3-dien-1-yl)nona-2,4,6,8-tetraenamide (37)

Compound **37** was synthesized using general procedure B. Yellow powder. Yield: 0.135 g (51%); mp: 110-112 °C; ^{1}H NMR (400 MHz, $CDCl_3$) δ 8.50 (dd, *J* = 4.8, 1.6 Hz, 1H), 8.47 (d, *J* = 1.5 Hz, 1H), 7.76 (d, *J* = 15.3 Hz, 1H), 7.56 – 7.50 (m, 1H), 7.05 (d, *J* = 8.4 Hz, 2H), 6.87 (dd, *J* = 15.3, 11.5 Hz, 1H), 6.80 (d, *J* = 8.5 Hz, 2H), 6.30 (d, *J* = 3.1 Hz, 2H), 6.27 (d, *J* = 11.3 Hz, 1H), 5.79 (t, *J* = 4.7 Hz, 1H), 5.53 (t, *J* = 5.6 Hz, 1H), 5.49 (s, 1H), 3.53 (dd, *J* = 12.9, 6.8 Hz, 2H), 2.77 (t, *J* = 6.9 Hz, 2H), 2.21 (d, *J* = 4.8 Hz, 2H), 2.00 (s, 6H), 1.71 (s, 3H), 1.09 (s, 6H). ^{13}C NMR (100 MHz, $CDCl_3$) δ 166.6, 154.8, 148.9, 147.5, 146.2, 141.8, 138.3, 138.2, 138.1, 137.8, 135.8, 131.7, 130.5, 130.4, 129.8, 126.3, 126.3, 126.2, 122.9, 120.1, 115.6, 40.7, 39.4, 34.8, 34.3, 26.6, 20.7, 18.9, 12.7; calcd for $C_{33}H_{38}N_2O_2Na^+$, 517.2803. Found: 517.2824.

(2*Z*,4*E*,6*E*,8*E*)-3,7-dimethyl-*N*-phenyl-9-(2,6,6-trimethyl-3-(pyrimidin-5-yl)cyclohexa-1,3-dien-1-yl)nona-2,4,6,8-tetraenamide (38).

Compound **38** was synthesized using general procedure B. Yellow powder. Yield: 0.116 g (48%); mp: 105-107 °C; ^{1}H NMR (400 MHz, $CDCl_3$) δ 9.12 (s, 1H), 8.61 (d, *J* = 6.1 Hz, 2H), 7.94 (d, *J* = 15.2 Hz, 1H), 7.54 (s, 2H), 7.32 (t, *J* = 7.9 Hz, 2H), 7.12 (dd, *J* = 18.8, 11.4 Hz, 2H), 6.96 (dd, *J* = 15.4, 11.5 Hz, 1H), 6.37 – 6.27 (m, 2H), 5.84 (t, *J* = 4.5 Hz, 1H), 5.69 (s, 1H), 2.24 (d, *J* = 4.7 Hz, 2H), 2.10 (s, 3H), 2.01 (d, *J* = 11.4 Hz, 3H), 1.72 (s, 3H), 1.11 (d, *J* = 6.6 Hz, 6H). ^{13}C NMR (100 MHz, $CDCl_3$) δ 166.3, 156.9, 156.8, 155.8, 155.3, 146.6, 142.7, 142.6, 138.6, 138.3, 138.1, 137.9, 135.5, 135.2, 132.1, 130.7, 130.5, 129.4, 127.9, 125.9, 125.1, 120.0, 115.5, 39.4, 34.3, 26.5, 20.7, 18.9, 12.7; calcd for $C_{30}H_{33}N_3ONa^+$, 474.2515. Found: 474.2515.

(2*Z*,4*E*,6*E*,8*E*)-*N*-(4-hydroxybenzyl)-3,7-dimethyl-9-(2,6,6-trimethyl-3-(pyrimidin-5-yl)cyclohexa-1,3-dien-1-yl)nona-2,4,6,8-tetraenamide (39)

Compound **39** was synthesized using general procedure B. Yellow powder. Yield: 0.154 g (60%); mp: 145-147°C; ^{1}H NMR (400 MHz, $CDCl_3$) δ 9.13 (s, 1H), 8.61 (d, *J* = 6.6 Hz, 2H), 7.84 (d, *J* = 15.3 Hz, 1H), 7.17 (d, *J* = 8.3 Hz, 2H), 6.87 (d, *J* = 15.3 Hz, 1H), 6.80 (d, *J* = 8.4 Hz, 2H), 6.28 (d, *J* = 5.2 Hz, 2H), 5.85 (t, *J* = 4.6 Hz, 1H), 5.70 (d, *J* = 11.4 Hz, 1H), 5.57 (s, 1H), 4.41 (d, *J* = 5.6 Hz, 2H), 2.24 (d, *J* = 4.8 Hz, 2H), 2.02 (d, *J* = 7.0 Hz, 6H), 1.72 (s, 3H), 1.10 (d, *J* = 5.7 Hz, 6H). ^{13}C NMR (100 MHz, $CDCl_3$) δ 166.3, 156.9, 156.8, 155.8, 155.3, 146.6, 142.7, 142.6, 138.6, 138.3, 138.1, 137.9, 135.5, 135.2, 132.1, 130.7, 130.5, 129.4, 127.9, 125.9, 125.1, 120.0, 115.5, 43.0, 39.4, 34.3, 26.5, 20.7, 18.9, 12.7; calcd for $C_{31}H_{35}N_3O_2Na^+$, 504.2621. Found: 504.2620.

(2*Z*,4*E*,6*E*,8*E*)-*N*-(4-hydroxyphenethyl)-3,7-dimethyl-9-(2,6,6-trimethyl-3-(pyrimidin-5-yl)cyclohexa-1,3-dien-1-yl)nona-2,4,6,8-tetraenamide (40)

Compound **40** was synthesized using general procedure B. Yellow powder. Yield: 0.161 g (61%); mp:115-117°C; ^{1}H NMR (400 MHz, $CDCl_3$) δ 9.12 (s, 1H), 8.61 (d, *J* = 3.5 Hz, 2H), 7.77 (d, *J* = 15.3 Hz, 1H), 7.05 (d, *J* = 8.3 Hz, 2H), 6.79 (d, *J* = 8.3 Hz, 2H), 6.32 – 6.21 (m, 2H), 5.84 (t, *J* = 4.6 Hz, 1H), 5.55 (t, *J* = 5.7 Hz, 1H), 5.50 (s, 1H), 3.53 (dd, *J* = 12.9, 6.7 Hz, 2H), 2.77 (t, *J* = 6.9 Hz, 2H), 2.24 (d, *J* = 4.8 Hz, 2H), 1.99 (d, *J* = 7.6 Hz, 6H), 1.74 (d, *J* = 10.0 Hz, 3H), 1.13 – 1.02 (m, 6H). ^{13}C NMR (100 MHz, $CDCl_3$) δ 166.6, 156.8, 155.8, 154.7, 146.3, 142.6, 138.5, 138.0, 135.5, 135.2, 132.0, 130.6, 130.5, 130.4, 129.8, 128.0, 125.9, 125.0, 120.2, 115.6, 40.7, 39.4, 34.8, 34.3, 26.6, 20.7, 18.8, 12.7; calcd for $C_{32}H_{37}N_3O_2Na^+$, 518.2777. Found: 518.2778.

Biology Experiments: Cell Culture:

Cell culture and Western blotting

MCF-7, MDA-MB-231, MDA-MB-468 and SKBR-3 human breast cancer cells and LNCaP, PC-3, and CWR22Rv1 human prostate carcinoma cells (American Type Culture Collection, Manassas, VA, USA) were maintained in RPMI 1640 media (Gibreast cancero-Life Technologies, Grand Island, NY, USA) supplemented with 10% fetal bovine serum and 1% penicillin/streptomycin. Western blotting was done as mentioned previously,[8, 13b] using the following antibodies: AR, Bad, Bax, Breast cancerl-2, eIF4E, Mnk1, Mnk-2, N-cadherin, PARP, peIF4E^{ser209} purchased from Cell Signaling Technology, Danvers, MA, USA. Anti-Mnk2 was purchased from Sigma-Aldrich and normal rabbit IgG, cyclin D1 was from Santa Cruz Biotechnology, CA, USA.

Cell proliferation analysis

Cells were plated (2500 cells/well) in 96 well plates and treated with or without specified compounds as described previously.[8a, 12b]

Wound healing assay

Wound healing assay was conducted as described previously using MDA-MB-231 and PC-3 cells following treatment with 5 μM of NRs for 24 h.[8a, 29]

siRNA transfection and luciferase assay

siRNA (100 nM) was transfected into LNCaP cells using Lipofectamine® 2000 Transfection reagent (Invitrogen) as per manufacturer's protocol. Protein silencing was confirmed by

immunoblot analysis. For cell growth assay experiments, transfection complex were removed after 18 h, cells were washed twice with PBS and replaced with growth medium. 24 h later drug was added and harvested after 72 h. For Western blot experiment, transfection complexes were washed off after 18 h and replaced with phenol free media for 24 h. Cells were then treated with 20 μM of compound 20 for an additional 24 h and cells were lysed using RIPA lysis buffer.[8b, 30] Luciferase assay was conducted in LNCaP cells using the Dual Luciferase kit (Promega) as described earlier.[8b, 13b]

***In Vivo* Anti-tumor Studies:**

All animal studies were performed according to the guidelines and approval of the Animal Care Committee of the University Of Maryland School Of Medicine, Baltimore. Female Athymic Nude mice or male SCID (Charles Rivers Laboratories or UMB facilities) at 4-6 weeks of age were maintained in a pathogen-free environment. MDA-MB-231 (10×10^6) breast cancer cells were subcutaneously implanted into Athymic Nude mice and CWR22Rv1 (1×10^6) cells into male SCID mice. Mice bearing established tumors (~100 mm^3) were randomized into treatment groups of 6 and dosed with vehicle (40% β-cyclodexdrin in ddH_2O), or compounds 20 and 22 (i.p., formulated in 40% β-cyclodexdrin in ddH_2O, once daily, 5 days a week for 28 days).

***In Vivo* Anti-tumor Activity:** We used the National Cancer Institute (NCI) criteria[24] to determine tumor growth efficacy of our compounds. Thus, percent test or treatment/control (%T/C), defined as the ratio of the median tumor volume for the treated group *vs.* control group was calculated as %T/C = [(median tumor volume of treated group at day 28)/(median tumor

volume of control group at day 28)] x 100. By this criteria, agents which confer %T/C <42% are considered minimally effective/active, and %T/C <10% are considered to be highly active.[24]

Statistical analysis

All experiments were carried out in at least triplicates and are expressed as mean ± S.E. where applicable. Treatments were compared to controls using the Student's t-test with either GraphPad Prism or Sigma Plot. Differences between groups were considered statistically significant at $P < 0.05$.

ASSOCIATED CONTENT

Supporting Information:

HPLC chromatograms and high resolution mass spectral data for compounds **16** – **20** and **33** – **40**. This material is available free of charge via the Internet at http://pubs.acs.org.

AUTHOR INFORMATION

Corresponding Author

*Phone: (410) 706 6364; Fax: (410) 706 0032; E-mail: vnjar@som.umaryland.edu

Author Contributions

#H.G.M, S.R., and V.P.R. contributed equally to the work performed in this manuscript.

Notes

The authors declare the following competing financial interest(s): Vincent C. O. Njar is the lead inventor of the novel compound disclosed in this manuscript and patents and technologies

thereof owned by the University of Maryland, Baltimore. The other authors, including Hannah W. Mbatia, Senthilmurugan Ramalingam, and Vidya P. Ramamurthy are also co-inventors on a pending patent to protect the novel compounds of this manuscript.

ACKNOWLEDGEMENTS

This work was supported by a grant from NIH and NCI (1RO1CA129379) and from start-up funds from University of Maryland School of Medicine and the Center for Biomolecular Therapeutics (CBT), Baltimore, USA to Professor Vincent C. O. Njar.

ABBREVIATIONS USED

AML, acute myeloid leukemia; AR, Androgen Receptor; AR-V7, type of slice variant AR; ATRA, all-trans retinoic acid; BC, breast cancer; eIF4E, eukaryotic translation initiation factor 4E; MAPK, mitogen activated protein kinase; fAR, full-length AR; Mnks, MAPK-interacting kinases; GI_{50}, concentration of agent/compound needed to inhibit cell growth by 50%.;MNKDAs, Mnk degrading agents; peIF4E, phosphorylated eukaryotic translation initiation factor 4E; NR, novel retinamides; PC, prostate cancer; TLC, thin layer chromatography; TNBC, triple negative breast cancer; 4-HPR, 4-hydroxyphenyl retinamide, 13-CRA, 13-cis-retinoic acid;

REFERENCES

1. (a) Avdulov, S.; Li, S.; Michalek, V.; Burrichter, D.; Peterson, M.; Perlman, D. M.; Manivel, J. C.; Sonenberg, N.; Yee, D.; Bitterman, P. B.; Polunovsky, V. A., Activation of translation complex eIF4F is essential for the genesis and maintenance of the malignant phenotype in human mammary epithelial cells. *Cancer Cell* **2004,** *5* (6), 553-563; (b) Gebauer, F.; Hentze, M. W., Molecular mechanisms of translational control. *Nat. Rev.. Mol. Cell Biol.* **2004,** *5* (10), 827-35; (c) Sonenberg, N.; Hinnebusch, A. G., Regulation of translation initiation in eukaryotes: mechanisms and biological targets. *Cell* **2009,** *136* (4), 731-745.

2. (a) Nasr, Z.; Robert, F.; Porco, J. A., Jr.; Muller, W. J.; Pelletier, J., eIF4F suppression in breast cancer affects maintenance and progression. *Oncogene* **2013,** *32* (7), 861-871; (b) Robichaud, N.; Del Rincon, S. V.; Huor, B.; Alain, T.; Petruccelli, L. A.; Hearnden, J.; Goncalves, C.; Grotegut, S.; Spruck, C. H.; Furic, L.; Larsson, O.; Muller, W. J.; Miller, W. H.; Sonenberg, N., Phosphorylation of eIF4E promotes EMT and metastasis via translational control of SNAIL and MMP-3. *Oncogene* **2014**; (c) Wendel, H. G.; Silva, R. L.; Malina, A.; Mills, J. R.; Zhu, H.; Ueda, T.; Watanabe-Fukunaga, R.; Fukunaga, R.; Teruya-Feldstein, J.; Pelletier, J.; Lowe, S. W., Dissecting eIF4E action in tumorigenesis. *Genes & development* **2007,** *21* (24), 3232-3237.

3. (a) Aktas, B. H.; Qiao, Y.; Ozdelen, E.; Schubert, R.; Sevinc, S.; Harbinski, F.; Grubissich, L.; Singer, S.; Halperin, J. A., Small-Molecule targeting of translation initiation for cancer therapy. *Oncotarget* **2013,** *4* (10), 1606-1617; (b) Bitterman, P. B.; Polunovsky, V. A., Attacking a nexus of the oncogenic circuitry by reversing aberrant eIF4F-mediated translation. *Mol. Cancer Ther.* **2012,** *11* (5), 1051-1061; (c) Bitterman, P.

B.; Polunovsky, V. A., Translational control of cell fate: from integration of environmental signals to breaching anticancer defense. *Cell Cycle* **2012,** *11* (6), 1097-1107; (d) Carroll, M.; Borden, K. L., The oncogene eIF4E: using biochemical insights to target cancer. *J. Interf. Cyto. Res.* **2013,** *33* (5), 227-238; (e) Diab, S.; Kumarasiri, M.; Yu, M.; Teo, T.; Proud, C.; Milne, R.; Wang, S., MAP kinase-interacting kinases-emerging targets against cancer. *Chem. Biol.* **2014,** *21* (4), 441-452.

4. Graff, J. R.; Konicek, B. W.; Vincent, T. M.; Lynch, R. L.; Monteith, D.; Weir, S. N.; Schwier, P.; Capen, A.; Goode, R. L.; Dowless, M. S.; Chen, Y.; Zhang, H.; Sissons, S.; Cox, K.; McNulty, A. M.; Parsons, S. H.; Wang, T.; Sams, L.; Geeganage, S.; Douglass, L. E.; Neubauer, B. L.; Dean, N. M.; Blanchard, K.; Shou, J.; Stancato, L. F.; Carter, J. H.; Marcusson, E. G., Therapeutic suppression of translation initiation factor eIF4E expression reduces tumor growth without toxicity. *J Clin. Invest.* **2007,** *117* (9), 2638-2648.

5. Hong, D. S.; Kurzrock, R.; Oh, Y.; Wheler, J.; Naing, A.; Brail, L.; Callies, S.; Andre, V.; Kadam, S. K.; Nasir, A.; Holzer, T. R.; Meric-Bernstam, F.; Fishman, M.; Simon, G., A phase 1 dose escalation, pharmacokinetic, and pharmacodynamic evaluation of eIF-4E antisense oligonucleotide LY2275796 in patients with advanced cancer. *Clin. Cancer Res.* **2011,** *17* (20), 6582-6591.

6. Konicek, B. W.; Stephens, J. R.; McNulty, A. M.; Robichaud, N.; Peery, R. B.; Dumstorf, C. A.; Dowless, M. S.; Iversen, P. W.; Parsons, S.; Ellis, K. E.; McCann, D. J.; Pelletier, J.; Furic, L.; Yingling, J. M.; Stancato, L. F.; Sonenberg, N.; Graff, J. R., Therapeutic inhibition of MAP kinase interacting kinase blocks eukaryotic initiation

factor 4E phosphorylation and suppresses outgrowth of experimental lung metastases. *Cancer Res.* **2011,** *71* (5), 1849-1857.

7. Altman, J. K.; Szilard, A.; Konicek, B. W.; Iversen, P. W.; Kroczynska, B.; Glaser, H.; Sassano, A.; Vakana, E.; Graff, J. R.; Platanias, L. C., Inhibition of Mnk kinase activity by cercosporamide and suppressive effects on acute myeloid leukemia precursors. *Blood* **2013,** *121* (18), 3675-3681.

8. (a) Ramalingam, S.; Gediya, L.; Kwegyir-Afful, A. K.; Ramamurthy, V. P.; Purushottamachar, P.; Mbatia, H.; Njar, V. C., First MNKs degrading agents block phosphorylation of eIF4E, induce apoptosis, inhibit cell growth, migration and invasion in triple negative and Her2-overexpressing breast cancer cell lines. *Oncotarget* **2014,** *5* (2), 530-543; (b) Ramamurthy, V. P., Ramalingam, S., Gediya, L. K., Kwegyir-Afful, A. K., Njar, V. C. O., Simultaneous targeting of AR and MNK signaling pathways by novel retinamides induce profound anti-tumor and anti-invasive activities in human prostate cancer cell lines. *Oncotarget* **2014**, in press.

9. Hou, J.; Lam, F.; Proud, C.; Wang, S., Targeting Mnks for cancer therapy. *Oncotarget* **2012,** *3* (2), 118-131.

10. Bain, J.; Plater, L.; Elliott, M.; Shpiro, N.; Hastie, C. J.; McLauchlan, H.; Klevernic, I.; Arthur, J. S.; Alessi, D. R.; Cohen, P., The selectivity of protein kinase inhibitors: a further update. *Biochem. J.* **2007,** *408* (3), 297-315.

11. Teo, T., Lam, F., Yu, M., Yang, Y., Basnet, S., Albrecht, H., Sykes, M., Wag, S., Pharmacologic inhibition of Mnks in acute myeloid leukemia. *FEBS J.* **2014,** *In press*.

12. (a) Njar, V. C.; Gediya, L.; Purushottamachar, P.; Chopra, P.; Vasaitis, T. S.; Khandelwal, A.; Mehta, J.; Huynh, C.; Belosay, A.; Patel, J., Retinoic acid metabolism

blocking agents (RAMBAs) for treatment of cancer and dermatological diseases. *Bioorg. Med. Chem.* **2006,** *14* (13), 4323-4340; (b) Patel, J. B.; Huynh, C. K.; Handratta, V. D.; Gediya, L. K.; Brodie, A. M.; Goloubeva, O. G.; Clement, O. O.; Nanne, I. P.; Soprano, D. R.; Njar, V. C., Novel retinoic acid metabolism blocking agents endowed with multiple biological activities are efficient growth inhibitors of human breast and prostate cancer cells in vitro and a human breast tumor xenograft in nude mice. *J. Med. Chem.* **2004,** *47* (27), 6716-6729.

13. (a) Bissantz, C.; Kuhn, B.; Stahl, M., A medicinal chemist's guide to molecular interactions. *J. Med. Chem.* **2010,** *53* (14), 5061-5084; (b) Purushottamachar, P.; Godbole, A. M.; Gediya, L. K.; Martin, M. S.; Vasaitis, T. S.; Kwegyir-Afful, A. K.; Ramalingam, S.; Ates-Alagoz, Z.; Njar, V. C., Systematic structure modifications of multitarget prostate cancer drug candidate galeterone to produce novel androgen receptor down-regulating agents as an approach to treatment of advanced prostate cancer. *J. Med. Chem.* **2013,** *56* (12), 4880-4898.

14. (a) Clamon, G.; Chabot, G. G.; Valeriote, F.; Davilla, E.; Vogel, C.; Gorowski, E.; Birch, R., Phase I study and pharmacokinetics of weekly high-dose 13-cis-retinoic acid. *Cancer Res.* **1985,** *45* (4), 1874-1878; (b) Reynolds, C. P.; Matthay, K. K.; Villablanca, J. G.; Maurer, B. J., Retinoid therapy of high-risk neuroblastoma. *Cancer Lett.* **2003,** *197* (1-2), 185-192; (c) Veal, G. J.; Cole, M.; Errington, J.; Pearson, A. D.; Foot, A. B.; Whyman, G.; Boddy, A. V.; Group, U. P. W., Pharmacokinetics and metabolism of 13-cis-retinoic acid (isotretinoin) in children with high-risk neuroblastoma - a study of the United Kingdom Children's Cancer Study Group. *Br. J. Cancer* **2007,** *96* (3), 424-431.

15. Marill, J.; Capron, C. C.; Idres, N.; Chabot, G. G., Human cytochrome P450s involved in the metabolism of 9-cis- and 13-cis-retinoic acids. *Biochem. Pharmacol.* **2002,** *63* (5), 933-943.

16. (a) Hu, Q.; Negri, M.; Jahn-Hoffmann, K.; Zhuang, Y.; Olgen, S.; Bartels, M.; Muller-Vieira, U.; Lauterbach, T.; Hartmann, R. W., Synthesis, biological evaluation, and molecular modeling studies of methylene imidazole substituted biaryls as inhibitors of human 17alpha-hydroxylase-17,20-lyase (CYP17)--part II: Core rigidification and influence of substituents at the methylene bridge. *Bioorg. Med. Chem.* **2008,** *16* (16), 7715-7727; (b) Mahalingam, P.; Takrouri, K.; Chen, T.; Sahoo, R.; Papadopoulos, E.; Chen, L.; Wagner, G.; Aktas, B. H.; Halperin, J. A.; Chorev, M., Synthesis of rigidified eIF4E/eIF4G inhibitor-1 (4EGI-1) mimetic and their in vitro characterization as inhibitors of protein-protein interaction. *J. Med. Chem.* **2014,** *57* (12), 5094-5111.

17. (a) Agranat, I.; Caner, H.; Caldwell, J., Putting chirality to work: the strategy of chiral switches. *Nat. Rev. Drug Dis.* **2002,** *1* (10), 753-768; (b) Caner, H.; Groner, E.; Levy, L.; Agranat, I., Trends in the development of chiral drugs. *Drug Dis. Today* **2004,** *9* (3), 105-110.

18. Johnson, A. T.; Klein, E. S.; Gillett, S. J.; Wang, L.; Song, T. K.; Pino, M. E.; Chandraratna, R. A. S., Synthesis and Characterization of a Highly Potent and Effective Antagonist of Retinoic Acid Receptors. *J. Med. Chem.* **1995,** *38*, 4764-4767.

19. Zaveri, N.; Jiang, F.; Olsen, C.; Polgar, W.; Toll, L., Novel α3β4 Nicotinic Acetylcholine Receptor-Selective Ligands. Discovery, Structure-Activity Studies, and Pharmacological Evaluation. *J. Med. Chem.* **2010,** *53*, 8187-8191.

20. Gediya, L. K.; Khandelwal, A.; Patel, J.; Belosay, A.; Sabnis, G.; Mehta, J.; Purushottamachar, P.; Njar, V. C., Design, synthesis, and evaluation of novel mutual prodrugs (hybrid drugs) of all-trans-retinoic acid and histone deacetylase inhibitors with enhanced anticancer activities in breast and prostate cancer cells in vitro. *J. Med. Chem.* **2008,** *51* (13), 3895-3904.

21. Lonergan, P. E.; Tindall, D. J., Androgen receptor signaling in prostate cancer development and progression. *J. Carcinogen.* **2011,** *10*, 20, doi: 10.4103/1477-3163.83937. Epub 2011 Aug 23.

22. Liao, X.; Tang, S.; Thrasher, J. B.; Griebling, T. L.; Li, B., Small-interfering RNA-induced androgen receptor silencing leads to apoptotic cell death in prostate cancer. *Mol. Cancer Ther.* **2005,** *4* (4), 505-515.

23. Malagarie-Cazenave, S.; Olea-Herrero, N.; Vara, D.; Diaz-Laviada, I., Capsaicin, a component of red peppers, induces expression of androgen receptor via PI3K and MAPK pathways in prostate LNCaP cells. *FEBS Lett.* **2009,** *583* (1), 141-147.

24. (a) Bissery, M. C.; Chabot, G. G., History and new development of screening and evaluation methods of anticancer drugs used in vivo and in vitro. *Bull. Cancer* **1991,** *78* (7), 587-602; (b) Hollingshead, M. G., Antitumor efficacy testing in rodents. *J. Natl. Cancer Inst.* **2008,** *100* (21), 1500-1510.

25. Ramalingam, S. G., L. K.; Ramamurthy, V. P.; Chen, H.; Lapidus, R.; Njar, V. C. O, Novel MNKDAs exert potent therapeutic effects against human breast cancer tumor growth and metastasis. 2015, unpublished results.

26. Njar, V. C.; Brodie, A. M., Discovery and development of galeterone (TOK-001 or VN/124-1) for treatment of all stages of prostate cancer. *J. Med. Chem.* **2015,** in press.

27. Hsieh, A. C.; Ruggero, D., Targeting eukaryotic translation initiation factor 4E (eIF4E) in cancer. *Clin. Cancer Res.* **2010,** *16* (20), 4914-4920.

28. Hagner, P. R.; Schneider, A.; Gartenhaus, R. B., Targeting the translational machinery as a novel treatment strategy for hematologic malignancies. *Blood* **2010,** *115* (11), 2127-2135.

29. Kanazawa, S.; Fujiwara, T.; Matsuzaki, S.; Shingaki, K.; Taniguchi, M.; Miyata, S.; Tohyama, M.; Sakai, Y.; Yano, K.; Hosokawa, K.; Kubo, T., bFGF regulates PI3-kinase-Rac1-JNK pathway and promotes fibroblast migration in wound healing. *PloS One* **2010,** *5* (8), e12228.

30. Grzmil, M.; Huber, R. M.; Hess, D.; Frank, S.; Hynx, D.; Moncayo, G.; Klein, D.; Merlo, A.; Hemmings, B. A., MNK1 pathway activity maintains protein synthesis in rapalog-treated gliomas. *J. Clin. Invest.* **2014,** *124* (2), 742-754.

TABLE OF CONTENT GRAPHIC